Spectral Efficiency of Multicarrier CDMA

Antonia M. Tulino, *Member, IEEE*, Linbo Li, and Sergio Verdú, *Fellow, IEEE*

***Abstract*—We analyze the spectral efficiency (sum-rate per subcarrier) of randomly spread synchronous multicarrier code-division multiple access (MC-CDMA) subject to frequency-selective fading in the asymptotic regime of number of users and bandwidth going to infinity with a constant ratio. Both uplink and downlink are considered, either conditioned on the subcarrier fading coefficients (for nonergodic channels) or unconditioned thereon (for ergodic channels). The following receivers are analyzed: a) jointly optimum receiver, b) linear minimum mean-square error (MMSE) receiver, c) decorrelator, and d) single-user matched filter.**

***Index Terms*—Channel capacity, multicarrier code-division multiple access (MC-CDMA), random matrix theory, multiuser information theory, fading channels.**

I. Introduction

A. Motivation

MULTICARRIER code-division multiple access (MC-CDMA) is a promising approach to the challenge of providing high data rate wireless communication. It represents the fusion of two distinct techniques.

- The first is orthogonal frequency-division multiplexing (OFDM), which addresses the intersymbol interference problem arising in channels where the signal bandwidth exceeds the coherence bandwidth of the fading process. The idea in OFDM is to divide the available bandwidth into a large number of small orthogonal bands or *subcarriers*, each much smaller that the coherence bandwidth and thus exposed only to frequency-flat fading. A central feature of OFDM is that it can take advantage of the fast Fourier transform (FFT) to translate the signal from the frequency to the time domain and *vice versa*.
- The second ingredient is CDMA, which has become a prominent multiple-access technique in mobile wireless systems. In its direct-sequence form, however, CDMA suffers in the face of frequency-selective fading, particularly in the downlink where orthogonal spreading codes are typically employed. The orthogonality is destroyed by the channel, which renders the codes mutually interfering.

MC-CDMA combines the benefits of CDMA with the natural robustness to frequency selectivity offered by OFDM. It can be interpreted as CDMA with the spreading taking place in the frequency rather than temporal domain.[1] In MC-CDMA, the processing and signature spreading occurs in the frequency domain. Optimum as well as linear receivers, such as the matched filter, decorrelator. and minimum mean-squared error (MMSE) can be used in the frequency domain in an analogous way to their use in the time domain for DS-CDMA.

The number of subcarriers in MC-CDMA is typically large enough to render the problem a very good candidate for the application of the theory of large random matrices. In this paper, using results on the eigenvalue distribution of such matrices, we investigate the spectral efficiency of several linear and nonlinear receivers for synchronous MC-CDMA in the presence of frequency-selective fading. The analysis is conducted in the usual asymptote where the number of users and degrees of freedom go to infinity with constant ratio. In MC-CDMA, the degrees of freedom are embodied by the different subcarriers.

Related asymptotic analyses of synchronous MC-CDMA with independent and identically distributed (i.i.d.) orthogonal signatures are presented in [5], [6], [3]. Specifically in [5], the signal-to-interference-and-noise ratio (SINR) at the output of an MMSE receiver with i.i.d. and isotropic signatures is analyzed in the case of a downlink with equal-power users while, in [6], the spectral efficiency of the optimum receiver for that same scenario is obtained in integral form invoking the optimality of MMSE reception with successive interference cancellation [32]. The downlink with unequal-power users is analyzed in [3] in terms of the SINR at the output of an MMSE receiver under the assumption that the users are partitioned into a finite number of classes, each having a distinct power.

B. Scope

Unlike previous works, we treat both uplink and downlink with unequal-power users considering four types of receivers: jointly optimum, linear MMSE, decorrelator, and single-user matched filter. For these receiving schemes, with user signatures known by the receiver and with perfect channel state information therein, we characterize performance measures such as spectral efficiency, multiuser efficiency, and output SINR. For each scheme, the asymptotic values of these measures are

Manuscript received June 19, 2003; revised July 26, 2004. This work was prepared through collaborative participation in the Communications and Networks Consortium sponsored by the U.S. Army Research Laboratory under the Collaborative Technology Alliance Program, Cooperative Agreement DAAD19-01-2-0011. The U.S. Government is authorized to reproduce and distribute reprints for Government purposes notwithstanding any copyright notation thereon. The views and conclusions contained in this document are those of the authors and should not be interpreted as representing the official policies, either expressed or implied, of the Army Research Laboratory or the U.S. Government.

A. M. Tulino is with the Universitá Federico II, 81125 Napoli, Italy (e-mail: atulino@ee.princeton.edu).

L. Li was with the Department of Electrical Engineering, Princeton University, Princeton, NJ 08544 USA. He is now with Qualcomm Inc, San Diego, CA 92121 USA (e-mail: linbol@qualcomm.com).

S. Verdú is with the Department of Electrical Engineering, Princeton University, Princeton, NJ 08544 USA (e-mail: verdu@ee.princeton.edu).

Communicated by G. Caire, Associate Editor for Communications.

Digital Object Identifier 10.1109/TIT.2004.840875

[1]Compared with direct-sequence CDMA (DS-CDMA), MC-CDMA is less vulnerable to delay spread but, in return, more vulnerable to Doppler spread, which tends to destroy the orthogonality between the subcarriers.

found as function of the number of users per subcarrier, the empirical distribution of the fading across the subcarriers, and the signal-to-noise ratio (SNR). We further analyze the behavior of the spectral efficiency as a function of the normalized energy per bit with emphasis in the low- and high-power regimes, where the expressions turn out to be remarkably insightful. Previous results from [14], [27], [29] on the asymptotic eigenvalue moments of certain large random matrices are critically involved.

As shall be evidenced, the downlink turns out to be simply a particular instance of the uplink where the signals intended for the several users experience the exact same fading. Moreover, this special case also coincides—asymptotically—with the statistically symmetric uplink setup, where the fading experienced by the different users is independent and statistically equivalent. Thus, our approach is to emphasize the analysis of the general uplink, from which the downlink and the statistically symmetric uplink are then easily obtained.

The analysis embraces frequency-selective fading channels both nonergodic and ergodic in the time domain. For the former, the analysis must be conditioned on the fading realization since average performance measures would have no operational meaning. For the latter, however, it is meaningful to average over the fading ensemble to obtain ergodic performance measures. The expressions of every instantaneous performance measure of interest (for a given choice of the transmit spreading signatures and a given fading realization) involve the spectrum of a matrix, composed at the receiver, containing those spreading signatures distorted by such fading. For finite numbers of users and subcarriers, this spectrum is a random function at two levels: the spreading signatures and the fading. As the number of users and subcarriers grows without bound,[2] two different scenarios are possible.

- If the fading is ergodic in the frequency domain, the randomness in the spectrum of the received signature matrix due to both the choice of the spreading signatures and the realization of the fading vanishes asymptotically and only the statistical properties of the signatures and fading remain. The various instantaneous performance measures, thus, converge asymptotically to nonrandom limits. It is then immaterial whether the channel is temporally ergodic or not
- If the fading is nonergodic in the frequency domain,[3] the randomness due to the choice of the spreading signatures still vanishes but the randomness associated with the realization of the fading process does not. Rather, the performance measures converge asymptotically to quantities that are functions of the fading realization. In this case, further averaging over the fading ensemble yields the ergodic asymptotic performance measures, which are meaningful if the fading is temporally ergodic. If it is not, then a more appropriate characterization is through the concept of outage, i.e., the probability that the performance measures for a given fading realization fall below some threshold.

With this backdrop, the main contributions of the paper are as follows.

- We find the asymptotic spectral efficiency and multiuser efficiency of synchronous uplink MC-CDMA channels with either temporally nonergodic or ergodic frequency-selective fading for linear and nonlinear receivers. The fading coefficients affecting the subcarriers of a given user are allowed to be arbitrarily distributed and correlated, constrained only such that their marginal distributions have finite moments. Although, in their full generality, the spectral efficiencies emerge as solutions of fixed-point equations (which can be solved numerically), explicit expressions are found for several channels of interest.
- For channels ergodic in frequency, we prove that all performance measures of interest converge almost surely to nonrandom limits.
- We show that the spectral efficiency of the optimum nonlinear receiver can be characterized compactly in terms of that of the optimum linear receiver. This represents a generalization of the corresponding relationship found in [23].
- Every uplink expression is specialized to the corresponding downlink. Besides providing better insight, these also provide, through a simple reinterpretation of certain quantities, useful particular expressions for the uplink scenario where users are statistically identical
- Tightly framing achievable performance, particular emphasis is placed on the regions of low and high normalized energy per bit.
- Low- and high-power expressions for the multiuser efficiency, parameterized by the effective number of active users per nonzero-power subcarrier (effective load factor), are also derived.
- Some of the performance measures are also evaluated for low and high effective load factors.

The paper is organized as follows. Section II lays down some necessary definitions and a key auxiliary result used throughout. In Section III, we introduce detailed models for uplink and downlink MC-CDMA. The four different receivers are analyzed in detail in Sections IV–VII.

Although the paper focuses on MC-CDMA, the methodology also applies to related schemes such as conventional OFDM [30]. Related analyses in the context of multiple-antenna communication can be found in [27], [28].

II. Definitions and Auxiliary Results

Definition 2.1: Given a vector $\boldsymbol{D} = [d_1, \ldots, d_N]$, its empirical distribution is

$$F_N(x) = \frac{1}{N} \sum_{i=1}^{N} \mathrm{u}(x - d_i) \tag{1}$$

[2]For each particular system design, the width of the subcarriers should be carefully chosen to strike a balance between the vulnerability to delay spread and to Doppler spread. The subcarriers must be narrow enough to experience an essentially flat frequency response yet wide enough to resist Doppler spread. Accordingly, as the number of subcarriers scales, the subcarrier width is held fixed and thus the overall signal bandwidth scales similarly.

[3]For instance, due to a finite number of physical propagation paths in the radio channel.

where $\mathrm{u}(\cdot)$ is the unit step function. If d_i represents the ith eigenvalue of a matrix $\boldsymbol{A}$, then $F_N(\cdot)$ is also termed the spectrum of $\boldsymbol{A}$. If $F_N(\cdot)$ converges as $N \to \infty$, its limit (asymptotic empirical distribution) is denoted by $F(\cdot)$.

Definition 2.2: Let $\boldsymbol{D}$ be an $N \times K$ random matrix whose (i,j)th entry is $D_{i,j}$ and denote by $\lfloor \cdot \rfloor$ the closest smaller integer. For $x \in [0,1]$, let $F_x(\cdot)$ be the limit as $N \to \infty$ of the empirical distribution of

$$\left[|D_{\lfloor xN \rfloor,1}|^2, \ldots, |D_{\lfloor xN \rfloor,K}|^2\right]$$

and, for $y \in [0, K/N]$, let $F_y(\cdot)$ be the limit as $N \to \infty$ of the empirical distribution of

$$\left[|D_{1,\lfloor yN \rfloor}|^2, \ldots, |D_{N,\lfloor yN \rfloor}|^2\right].$$

As $N, K \to \infty$ with $K/N \to \beta$, the two-dimensional channel profile function of $\boldsymbol{D}$ is defined as

$$\rho_{\boldsymbol{D}}(x,y) : [0,1] \times [0,\beta] \to \mathbb{R} \tag{2}$$

such that, if X is uniform in $[0,1]$, the distribution of $\rho_{\boldsymbol{D}}(\mathsf{X}, y)$ equals $F_y(\cdot)$, and, if Y is uniform in $[0,1]$, the distribution of $\rho_{\boldsymbol{D}}(x, \mathsf{Y})$ equals $F_x(\cdot)$.

Furthermore, for a given column $k \in \{1, \ldots K\}$, the one-dimensional channel profile function of $[D_{1,k}, \ldots, D_{N,k}]$ is defined as

$$\rho_{\boldsymbol{D},k}(x) : [0,1] \to \mathbb{R} \tag{3}$$

such that, if X is uniform in $[0,1]$, the distribution of $\rho_{\boldsymbol{D},k}(\mathsf{X})$ equals the asymptotic empirical distribution of $[|D_{1,k}|^2, \ldots, |D_{N,k}|^2]$.

From the definition, it follows that

$$\frac{1}{\beta} \int_0^\beta \int_0^1 \rho_{\boldsymbol{D}}(x,y) dx dy = \lim_{K,N \to \infty} \frac{\|\boldsymbol{D}\|^2}{KN} \tag{4}$$

where $\|\cdot\|$ denotes the Frobenius norm, i.e., $\|\boldsymbol{D}\|^2 = \mathrm{Tr}\{\boldsymbol{D}\boldsymbol{D}^\dagger\}$.

Note that, in general, both the one-dimensional and the two-dimensional channel profile functions depend on the specific realization of $\boldsymbol{D}$. In some cases, however, that is not the case.

Definition 2.3: The $N \times K$ random matrix $\boldsymbol{D}$ is doubly ergodic if the asymptotic empirical distributions $F_x(\cdot)$ and $F_y(\cdot)$ in Definition 2.2 are almost surely nonrandom limits.

Remark 2.1: Given $k \in \{1, \ldots K\}$, for $[D_{1,k}, \ldots, D_{N,k}]$ with channel profile function $\rho_{\boldsymbol{D},k}(x)$ and asymptotic empirical distribution $F_k(\cdot)$, it is verified that

$$\int_0^1 g(\rho_{\boldsymbol{D},k}(x)) dx = \mathrm{E}[g(\Lambda)] \tag{5}$$

where g is any integrable function while $\mathrm{E}[\cdot]$ denotes the expectation with respect to the random variable Λ whose cumulative distribution is given by $F_k(\cdot)$.

The next theorem is a reformulation of the celebrated Girko's theorem [8], [10], [24] which has found several interesting applications in the contexts of wireless communications [4], [12].

Theorem 2.1: [14], [29] Consider an $N \times K$ matrix $\boldsymbol{V} = \boldsymbol{B} \circ \boldsymbol{D}$ with $\circ$ denoting Hadamard (element-wise) product and with $\boldsymbol{B}$ and $\boldsymbol{D}$ independent $N \times K$ random matrices. The entries of $\boldsymbol{B}$ are zero-mean i.i.d. complex, arbitrarily distributed, and with variance $1/N$, while $\boldsymbol{D}$ is as in Definition 2.2 with $F_x(\cdot)$ and $F_y(\cdot)$ having all their moments bounded. Denoting by $\rho_{\boldsymbol{D}}(\cdot,\cdot)$ the channel profile function of $\boldsymbol{D}$, then, as $K, N \to \infty$ with $K/N \to \beta$, the empirical eigenvalue distribution of $\boldsymbol{V}\boldsymbol{V}^\dagger$ converges almost surely, conditioned on $\boldsymbol{D}$, to a nonrandom distribution function whose Stieltjes transform is

$$\begin{aligned} \mathcal{S}_{\boldsymbol{V}}(z) &= \lim_{N \to \infty} \frac{1}{N} \mathrm{Tr} \left\{ \left(\boldsymbol{I} + z \boldsymbol{V}\boldsymbol{V}^\dagger \right)^{-1} \right\} \\ &= \int_0^1 v(x,z) dx \end{aligned} \tag{6}$$

with $v(\cdot, z)$ solution to the fixed-point equation

$$v(x,z) = \frac{1}{1 + z \int_0^\beta \frac{\rho_{\boldsymbol{D}}(x,y)}{1 + z \int_0^1 v(w,z) \rho_{\boldsymbol{D}}(w,y) dw} dy}. \tag{7}$$

In general, $\mathcal{S}_{\boldsymbol{V}}(\cdot)$ and consequently, the asymptotic empirical eigenvalue distribution of $\boldsymbol{V}\boldsymbol{V}^\dagger$ depend on the specific realization of $\boldsymbol{D}$. If $\boldsymbol{D}$ is doubly ergodic, then its channel profile function $\rho_{\boldsymbol{D}}(\cdot,\cdot)$ does not depend on the specific realization thereof and the empirical eigenvalue distribution of $\boldsymbol{V}\boldsymbol{V}^\dagger$ converges almost surely to a nonrandom limit whose Stieltjes transform is given by (6).

III. System Model

In MC-CDMA, there are N evenly spaced subcarriers shared by every user with N the spreading gain. Each symbol of the data stream generated by user k is replicated into N parallel copies. Each copy is then multiplied by a chip from the corresponding spreading signature and modulated onto one of the subcarriers, all of which are to be transmitted in parallel. The usual implementation calls for an inverse discrete Fourier transform (IDFT) to convert the N parallel chips into serial form for transmission. A cyclic prefix is appended to remove the interference between successive symbols and to accommodate the circulant convolution provided by the FFT at the expense of some loss in efficiency that can be easily incorporated as a penalty factor.

Denote by $\boldsymbol{S} = [\boldsymbol{s}_1, \ldots, \boldsymbol{s}_K]$ the $N \times K$ signature matrix whose kth column $\boldsymbol{s}_k$ represents the frequency-domain transmit signature of the kth user. The baseband signal transmitted by the kth user in the time domain is then $\boldsymbol{W}\boldsymbol{s}_k b_k$ where b_k is the data symbol of user k, unit-variance and i.i.d. across users, and $\boldsymbol{W}$ denotes the $N \times N$ IDFT matrix. The matrix $\boldsymbol{S}$ has i.i.d. entries with common mean and variance $\frac{1}{N}$. We will show that, asymptotically, both the conditioned and the ergodic performance measures for the various receivers do not depend on the choice of the signatures.

The receiver front-end consists of N matched filters, one for each subcarrier, which on the discrete baseband domain is equivalent to performing a discrete Fourier transform (DFT).

At the output, the received vector corresponding to the kth user in the frequency domain is $b_k\tilde{\boldsymbol{s}}_k$ where

$$\tilde{\boldsymbol{s}}_k = A_k \operatorname{diag}\left\{H_k^1,\ldots,H_k^N\right\}\boldsymbol{s}_k$$

with H_k^i the fading coefficient at the ith subcarrier of user k. These random fading coefficients model the short-term fading experienced by user k at each subcarrier while the deterministic parameter A_k captures the long-term attenuation due to range, shadow fading, etc., which does not vary substantially over the time scale of interest to us. In the case that the channel is *unfaded*, then $H_k^i = 1\ \forall\, i,k$ and thus the channel is completely determined by the A_k's. Notice that the IDFT and DFT operations and the role of the cyclic prefix are implicitly absorbed through the diagonal structure of the channel response.

Since, with frequency-flat fading, the analysis of MC-CDMA is mathematically equivalent to that of DS-CDMA [23], we directly focus on the more general case of frequency-selective fading. It is important to remark that, although the fading is allowed to be frequency selective, each subcarrier is narrow enough to experience only flat fading. Moreover, in order to ensure sustained robustness to Doppler as the number of subcarriers grows, the width of each subcarrier is held fixed while the overall signal bandwidth is allowed to scale with N.

For each user, the fading coefficients at different subcarriers are allowed to be correlated and arbitrarily (but identically) marginally distributed. Denoting by Δ_f the frequency spacing between two adjacent subcarriers, the correlation matrix $\boldsymbol{M}^{(k)}$ of the kth user's fading coefficients is given by [13], [21]

$$\begin{aligned}\boldsymbol{M}_{p,q}^{(k)} &= \mathbb{E}\left[H_k^p H_k^{q*}\right] = \int_{-\infty}^{+\infty}\phi_k(\tau)e^{-j2\pi\tau(p-q)\Delta_f}d\tau \\ &= \Phi_k\left((p-q)\Delta_f\right)\end{aligned} \tag{8}$$

with $\phi_k(\cdot)$ and $\Phi_k(\cdot)$, respectively, the power-delay response and the frequency correlation function of the channel for the kth user. The latter satisfies $\Phi_k(0) = 1\ \forall\, k$. As $N\to\infty$, the bandwidth of the signal increases and hence, for a given coherent bandwidth

$$\mathbb{E}\left[H_k^{p+\delta}H_k^{p*}\right] = \Phi_k(\delta\Delta_f)$$

vanishes as $\delta\to\infty$.

A. Uplink

Assuming user synchronicity, the uplink front-end receiver output in the frequency domain is

$$\begin{aligned}\boldsymbol{r} &= \sum_{k=1}^{K} A_k b_k \operatorname{diag}\left\{H_k^1,\ldots,H_k^N\right\}\boldsymbol{s}_k + \boldsymbol{n} \\ &= (\boldsymbol{H}\boldsymbol{A}\circ\boldsymbol{S})\boldsymbol{b} + \boldsymbol{n} \\ &= \tilde{\boldsymbol{S}}\boldsymbol{b} + \boldsymbol{n}\end{aligned} \tag{9}$$

where $\boldsymbol{n}$ is circularly symmetric complex Gaussian noise with $\mathrm{E}[\boldsymbol{n}\boldsymbol{n}^\dagger] = \sigma^2\boldsymbol{I}$ while $\boldsymbol{b} = [b_1,\ldots,b_K]$, $\boldsymbol{A} = \operatorname{diag}\{A_1,\ldots,A_K\}$, and $\tilde{\boldsymbol{S}} = [\tilde{\boldsymbol{s}}_1,\ldots,\tilde{\boldsymbol{s}}_K]$. In turn, $\boldsymbol{H}$ is an $N\times K$ matrix whose (i,k)th entry is H_k^i. In the uplink, the H_k^i's are always independent across users due to their different locations and thus the columns of $\boldsymbol{H}$ are independent. Define the *asymptotic* received energy per user as

$$\begin{aligned}Q &= \lim_{K\to\infty}\frac{1}{K}\sum_{k=1}^{K}\|\tilde{\boldsymbol{s}}_k\|^2 \\ &\overset{\text{a.s.}}{=} \lim_{K,N\to\infty}\frac{\|\boldsymbol{H}\boldsymbol{A}\|^2}{KN}\end{aligned} \tag{10}$$

where the convergence is almost surely (a.s.) conditioned on the fading. From (10) we can further define the received SNR as

$$\mathsf{snr} = \frac{Q}{\sigma^2}. \tag{11}$$

The performance measures that we seek to analyze depend only on the eigenvalues of $\tilde{\boldsymbol{S}}$, which has two distinct sources of randomness: i) the random signatures within $\boldsymbol{S}$, and ii) the fading in $\boldsymbol{H}$. Denote by $\rho(x,y)$, with $(x,y)\in[0,1]\times[0,\beta]$, the two-dimensional channel profile function of $\frac{1}{\sqrt{Q}}\boldsymbol{H}\boldsymbol{A}$. Note that x and y can be interpreted as the normalized (by the number of dimensions N) subcarrier and user indices, respectively. From (10) it follows that

$$\int_0^\beta\int_0^1 \rho(x,y)dxdy = \beta. \tag{12}$$

As $N,K\to\infty$, it follows from Theorem 2.1 that the empirical eigenvalue distribution of $\tilde{\boldsymbol{S}}\tilde{\boldsymbol{S}}^\dagger$ converges to a distribution function whose Stieltjes transform is given by (6) and (7) and with the role of $\rho_{\boldsymbol{D}}(\cdot,\cdot)$ played by $Q\rho(\cdot,\cdot)$. The asymptotic empirical eigenvalue distribution function of $\tilde{\boldsymbol{S}}\tilde{\boldsymbol{S}}^\dagger$ is therefore a sole functional of $Q\rho(\cdot,\cdot)$ that, in general, depends on the specific channel realization.[4] Hence, the randomness in the eigenvalues of $\tilde{\boldsymbol{S}}\tilde{\boldsymbol{S}}^\dagger$ associated with $\boldsymbol{S}$ vanishes asymptotically while the randomness that arises from fading remains and is captured by the random field $Q\rho(\cdot,\cdot)$.

If $\boldsymbol{H}$ is doubly ergodic, as per Definition 2.3, then $Q\rho(\cdot,\cdot)$ no longer depends on the realization of $\boldsymbol{H}$ and the empirical eigenvalue distribution of $\tilde{\boldsymbol{S}}\tilde{\boldsymbol{S}}^\dagger$, of which the instantaneous performance measures of interest are deterministic functions, converges almost surely to a nonrandom limit. Consequently, the instantaneous performance measures themselves converge almost surely to nonrandom limits and thus the asymptotic expressions for the performance measures conditioned on the fading (i.e., indicative of outages) coincide with their unconditioned (i.e., ergodic) counterparts. Thus, although throughout Sections IV–VII such expressions are presented conditioned on the fading, their applicability to the doubly ergodic case is immediate. Since the fading for different users is always independent, a necessary and sufficient condition for double ergodicity is that the empirical distribution of the subcarrier fading coefficients for every user converges almost surely to a nonrandom limit. We shall refer to this condition as ergodicity in frequency.

[4]Precisely, $\rho(\cdot,\cdot)$ is defined through the asymptotic empirical distribution of the columns and rows of $\frac{1}{Q}(\boldsymbol{H}\circ\boldsymbol{H})\boldsymbol{A}\boldsymbol{A}^\dagger$.

B. Downlink

In the downlink, every user's signal experiences the same fading. Hence, if the subcarrier fading coefficients are $H^1, \ldots, H^N$, the output of the front-end in (9) becomes

$$\boldsymbol{r} = \tilde{\boldsymbol{S}}\boldsymbol{b} + \boldsymbol{n} \tag{13}$$

where $\tilde{\boldsymbol{S}} = \boldsymbol{H}\boldsymbol{A} \circ \boldsymbol{S}$ with $\boldsymbol{H} = \mathbf{1}_K^T \otimes [H^1, \ldots, H^N]^T$ where $\otimes$ denotes Kronecker product while $\mathbf{1}_K$ is a K-dimensional column vector whose entries equal 1. The average received energy then factors as

$$Q = \underbrace{\left(\lim_{K\to\infty} \frac{1}{K}\sum_{k=1}^{K} |A_k|^2\right)}_{Q_y}\underbrace{\left(\lim_{N\to\infty} \frac{1}{N}\sum_{i=1}^{N} |H_i|^2\right)}_{Q_x}. \tag{14}$$

Applying again Theorem 2.1, the structure of $\boldsymbol{H}$ results in a channel profile function of $\frac{1}{\sqrt{Q}}\boldsymbol{H}\boldsymbol{A}$ that also factors as

$$\rho(x,y) = \frac{1}{Q}\rho_{\boldsymbol{H}}(x)\rho_{\boldsymbol{A}}(y) \tag{15}$$

with $(x,y) \in [0,1] \times [0,\beta]$. Substituting (15) in the asymptotic uplink expressions and using the integral relation given in (5), the asymptotic uplink performance measures specialize into simpler forms that provide enhanced engineering insight. Interestingly, this special form of the asymptotic results is also applicable to the uplink whenever the joint distribution of the subcarrier fading coefficients is identical for each user and the fading process is ergodic in frequency, a scenario that we term *statistical symmetry*.

As in the uplink, the randomness associated with $\boldsymbol{S}$ vanishes asymptotically whereas the randomness associated with the fading vanishes in the presence of ergodicity in the frequency domain, in which case the performance measure expressions conditioned on the fading (related to outages) in Sections IV–VII coincide with their ergodic counterparts.

IV. Linear MMSE Receiver

We start by considering a linear MMSE receiver, which maximizes the output SINR, followed by single-user decoders. For user k, the receiver is

$$\boldsymbol{c}_k^{\mathsf{mmse}} = \left(\tilde{\boldsymbol{S}}_k\tilde{\boldsymbol{S}}_k^{\dagger} + \sigma^2\boldsymbol{I}\right)^{-1}\tilde{\boldsymbol{s}}_k \tag{16}$$

where $\tilde{\boldsymbol{S}}_k = (\tilde{\boldsymbol{s}}_1, \ldots, \tilde{\boldsymbol{s}}_{k-1}, \tilde{\boldsymbol{s}}_{k+1}, \ldots, \tilde{\boldsymbol{s}}_K)$. The instantaneous output SINR is

$$\mathsf{SINR}_k = \tilde{\boldsymbol{s}}_k^{\dagger}\left(\tilde{\boldsymbol{S}}_k\tilde{\boldsymbol{S}}_k^{\dagger} + \sigma^2\boldsymbol{I}\right)^{-1}\tilde{\boldsymbol{s}}_k. \tag{17}$$

The instantaneous MMSE multiuser efficiency of user k, denoted by η_k^N, equals the ratio of SINR_k to the corresponding SNR in the absence of multiple-access interference (MAI) [33]

$$\eta_k^N = \frac{\sigma^2}{||\tilde{\boldsymbol{s}}_k||^2}\mathsf{SINR}_k \tag{18}$$

which measures the ability to suppress MAI.

A. Uplink

Recall that H_k^i is the fading coefficient at the ith subcarrier of user k, A_k is the long-term attenuation of user k, and $\rho(x,y)$, with $(x,y) \in [0,1] \times [0,\beta]$, is the two-dimensional channel profile function of $\frac{1}{\sqrt{Q}}\boldsymbol{H}\boldsymbol{A}$ with Q as defined in (10). The one-dimensional channel profile function of the kth column of $\frac{1}{\sqrt{Q}}\boldsymbol{H}\boldsymbol{A}$ is denoted by $\rho_k(x)$ with $x \in [0,1]$. In a system achieving spectral efficiency C, the normalized received energy per bit is [23]

$$\frac{E_b}{N_0} = \frac{\beta\mathsf{snr}}{\mathsf{C}} \tag{19}$$

while the normalized transmitted energy per bit is

$$\frac{E_b^t}{N_0} = \frac{\beta}{\sigma^2\mathsf{C}}. \tag{20}$$

Theorem 4.1: Conditioned on the fading coefficients, the instantaneous MMSE multiuser efficiency of user k converges as $K, N \to \infty$ with $K/N \to \beta$ almost surely to

$$\eta_k = \frac{\int_0^1 \rho_k(x)v(x,\mathsf{snr})dx}{\int_0^1 \rho_k(x)dx} \tag{21}$$

where $v(\cdot, \mathsf{snr})$ is the solution to

$$v(x,\mathsf{snr}) = \frac{1}{1+\mathsf{snr}\int_0^{\beta}\frac{\rho(x,y)}{1+\mathsf{snr}\int_0^1 v(w,\mathsf{snr})\rho(w,y)dw}dy}. \tag{22}$$

Proof: In the Appendix, Part A.

Recall from Section III that, with frequency ergodicity, $\rho_k(\cdot)$ and $\rho(\cdot,\cdot)$ do not depend on the fading realization and thus (21) and (22) also provide the ergodic MMSE multiuser efficiency. The same consideration holds for all the other theorems presented in this and in successive sections.

Note that, denoting by y' the normalized (by N) index of the kth user, the asymptotic value of the MMSE multiuser efficiency can be rewritten as

$$\eta_k = \frac{\int_0^1 \rho(x,y')v(x,\mathsf{snr})dx}{\int_0^1 \rho(x,y')dx}. \tag{23}$$

Theorem 4.2: Conditioned on the fading coefficients, the spectral efficiency (in bits per second per hertz (bits/s/Hz)) of the MMSE receiver converges almost surely to

$$\mathsf{C}^{\mathsf{mmse}} = \int_0^{\beta}\log_2\left(1+\mathsf{snr}\mu(y',\mathsf{snr})\right)dy' \tag{24}$$

where $\mu(y',\mathsf{snr})$ is the solution to

$$\mu(y',\mathsf{snr}) = \int_0^1 \frac{\rho(x,y')}{1+\mathsf{snr}\int_0^{\beta}\frac{\rho(x,y)}{1+\mathsf{snr}\mu(y,\mathsf{snr})}dy}dx. \tag{25}$$

Proof: As discussed in [23], the asymptotic normality of the MAI at the output of the MMSE receiver yields that the asymptotic linear MMSE spectral efficiency is

$$\mathsf{C}^{\mathsf{mmse}} = \lim_{K\to\infty}\frac{\beta}{K}\sum_{k=1}^{K}\log_2\left(1+\mathsf{SINR}_k\right). \tag{26}$$

Conditioned on the fading coefficients, from [1, Lemma 2.7]

$$||\tilde{\boldsymbol{s}}_k||^2 = A_k^2\boldsymbol{s}^{\dagger}\,\mathrm{diag}\left\{|H_k^1|^2, \ldots, |H_k^N|^2\right\}\boldsymbol{s} \xrightarrow{\text{a.s.}} Q\int_0^1 \rho_k(x)dx \tag{27}$$

and, using the definition of η_k

$$\mathsf{SINR}_k = \frac{\|\tilde{\boldsymbol{s}}_k\|^2}{\sigma^2}\eta_k. \tag{28}$$

Thus, (26) can be rewritten as

$$\mathsf{C}^{\mathsf{mmse}} = \lim_{K\to\infty}\frac{1}{N} \cdot \sum_{k=1}^{K}\log_2\left(1+\mathsf{snr}\int_0^1 \rho_k(x)v(x,\mathsf{snr})dx\right) \tag{29}$$

$$= \int_0^\beta \log_2\left(1+\mathsf{snr}\mu(y',\mathsf{snr})\right)dy' \tag{30}$$

where $\rho_k(\cdot)$ equals the one-dimensional channel profile function of $\frac{A_k}{\sqrt{Q}}\left[H_k^1,\ldots,H_k^N\right]$, $v(\cdot,\mathsf{snr})$ satisfies (22), y' denotes the normalized user index, and $\mu(y',\mathsf{snr})$, using (21)–(23), is the solution to (25). □

Notice from (21) that the function $\mu(y',\mathsf{snr})$ is proportional, through the square norm per dimension of the kth column of $\frac{1}{\sqrt{Q}}\boldsymbol{HA}$, to the multiuser efficiency of the kth user (whose normalized index, recall, is y'). Furthermore, $\mathsf{snr}\mu(y',\mathsf{snr})$ represents—as evidenced by (26)—the effective SINR of the kth user at the output of an MMSE receiver.

Note also that, using (22) and

$$\mu(y',\mathsf{snr}) = \int_0^1 \rho(x,y')v(x,\mathsf{snr})dx$$

we obtain the alternative fixed-point equation

$$\int_0^\beta \frac{\mathsf{snr}\mu(y,\mathsf{snr})}{1+\mathsf{snr}\mu(y,\mathsf{snr})}dy = 1-\int_0^1 \frac{1}{1+\mathsf{snr}\int_0^\beta \frac{\rho(x,y)}{1+\mathsf{snr}\mu(y,\mathsf{snr})}dy}dx \tag{31}$$

which is useful to derive some of the properties of the function $\mu(\cdot,\mathsf{snr})$ that we uncover next.

Property 4.1: If the channel is ergodic in frequency, then frequency-selective fading can only reduce the function $\mu(\cdot,\mathsf{snr})$ with respect to the corresponding unfaded channel.

To verify this property, note that for channels ergodic in frequency

$$\int_0^1 \rho(x,y)dx = |A_{\lfloor yN\rfloor}|^2/Q_y$$

with y the normalized user index and Q_y defined in (14). Note also that the left-hand side of (31) is monotonically increasing in $\mu(\cdot,\mathsf{snr})$. Then, apply Jensen's inequality to the expectation of the concave function on the right-hand side of the equality. The reduction of $\mu(\cdot,\mathsf{snr})$ results, in turn, in a reduction in the MMSE spectral efficiency with respect to the case of no fading.

Property 4.2: The behavior of $\mu(\cdot,\mathsf{snr})$ at low snr is

$$\mu(y',\mathsf{snr}) = \int_0^1 \rho(x,y')dx - \mathsf{snr}\int_0^1\int_0^\beta \rho(x,y')\rho(x,y)dydx + \mathsf{snr}^2\int_0^1 \rho(x,y')a(x)dx + o(\mathsf{snr}^2) \tag{32}$$

where

$$a(x) = \left(\int_0^\beta \rho(x,y)dy\right)^2 + \int_0^1\int_0^\beta \rho(x',y)\rho(x,y)dydx'. \tag{33}$$

Property 4.2 is proved by expanding the right-hand side of (25) in a series in snr.

In order to state Property 4.3, it is useful to define respective auxiliary parameters Z_X and Z_Y as

$$Z_X = \int_0^1 1\left\{\int_0^\beta \rho(x,y)dy \neq 0\right\}dx \tag{34}$$

$$Z_Y = \int_0^\beta 1\left\{\int_0^1 \rho(x,y)dx \neq 0\right\}dy \tag{35}$$

where $1\{\cdot\}$ is the indicator function. Using two auxiliary independent random variables X and Y, uniform in $[0,1]$ and $[0,\beta]$, respectively, Z_X and Z_Y can be rewritten as[5]

$$Z_X = \Pr\{\mathcal{Z}_X(\mathsf{X})\neq 0\} \quad Z_Y = \beta\Pr\{\mathcal{Z}_Y(\mathsf{Y})\neq 0\} \tag{36}$$

with

$$\mathcal{Z}_X(x) = \int_0^\beta \rho(x,y)dy \quad \mathcal{Z}_Y(y) = \int_0^1 \rho(x,y)dx. \tag{37}$$

Consequently, Z_X represents the fraction of subcarriers that are active while Z_Y represents β times the portion of users that are actively transmitting. Thus,

$$\beta' = \frac{Z_Y}{Z_X} = \beta\frac{\Pr\{\mathcal{Z}_Y(\mathsf{Y})\neq 0\}}{\Pr\{\mathcal{Z}_X(\mathsf{X})\neq 0\}} \tag{38}$$

can be viewed as the effective load of the system.

Property 4.3:

$$\lim_{\mathsf{snr}\to\infty}\mu(y',\mathsf{snr}) = \begin{cases}\theta(y'), & \beta'<1\\ 0, & \beta'\geq 1\end{cases} \tag{39}$$

where $\theta(y')$ is the positive solution to

$$\theta(y') = \int_0^1 \frac{\rho(x,y')}{1+\int_0^\beta \frac{\rho(x,y)}{\theta(y)}dy}dx. \tag{40}$$

Proof: In the Appendix, Part B.

Given the relationship between $\mu(\cdot,\mathsf{snr})$ and the multiuser efficiency, Property 4.3 relates to the fact that the limit for $\mathsf{snr}\to\infty$ of the multiuser efficiency of the kth user yields the energy of the projection of kth user's received signature onto the signal subspace that is free from MAI, i.e., its orthogonal complement. The dimension of such subspace equals $1-\beta'$ since β' indicates the fraction of dimensions on which active transmissions take place. If $\beta'\geq 1$, then there are no dimensions free of MAI and hence $\lim_{\mathsf{snr}\to\infty}\mu(\cdot,\mathsf{snr}) = 0$.

Property 4.4:

$$\lim_{\mathsf{snr}\to\infty}\mathsf{snr}\mu(y',\mathsf{snr}) = \begin{cases}\infty, & \beta'\leq 1 \text{ and } \mathcal{Z}_y(y')>0\\ \theta_1(y'), & \beta'>1 \text{ and } \mathcal{Z}_y(y')>0\\ 0, & \mathcal{Z}_y(y')=0\end{cases} \tag{41}$$

[5]Recall once again that, in general, $\rho(x,y)$ depends on the fading realization and consequently so do Z_X and Z_Y.

where $\theta_1(y')$ satisfies

$$\theta_1(y') = \int_0^1 \frac{\rho(x,y')dx}{\int_0^\beta \frac{\rho(x,y)}{1+\theta_1(y)}dy}. \tag{42}$$

Proof: In the Appendix, Part C.

Property 4.5: If $\mathcal{Z}_Y(y') > 0$ then

$$\lim_{\mathsf{snr}\to\infty} \frac{\mathsf{snr}\dot{\mu}(y',\mathsf{snr})}{\mu(y',\mathsf{snr})} = \begin{cases} 0, & \beta' < 1 \\ -\frac{1}{2}, & \beta' = 1 \\ -1, & \beta' > 1 \end{cases} \tag{43}$$

otherwise,

$$\lim_{\mathsf{snr}\to\infty} \frac{\mathsf{snr}\dot{\mu}(y',\mathsf{snr})}{\mu(y',\mathsf{snr})} = 0.$$

Proof: In the Appendix, Part D.

Note that the behavior at high SNR is largely determined by the effective system load β'.

The above properties are useful at evaluating the key performance measures in the low- and high-SNR regimes. Specifically, the minimum received normalized energy per bit required for reliable communication by an MMSE receiver is [23]

$$\frac{E_b}{N_0}_{\min} = \lim_{\mathsf{snr}\to 0} \frac{\beta\mathsf{snr}}{\mathsf{C}^{\mathsf{mmse}}(\mathsf{snr})}. \tag{44}$$

Since

$$\lim_{\mathsf{snr}\to 0} \frac{\mathsf{C}^{\mathsf{mmse}}(\mathsf{snr})}{\mathsf{snr}} = \dot{\mathsf{C}}^{\mathsf{mmse}}(0)$$

using Property 4.2

$$\frac{E_b}{N_0}_{\min} = \frac{\beta \log_e 2}{\lim_{\mathsf{snr}\to 0}\int_0^\beta \frac{\mu(y',\mathsf{snr})+\mathsf{snr}\dot{\mu}(y',\mathsf{snr})}{1+\mathsf{snr}\mu(y',\mathsf{snr})}dy'} \tag{45}$$

$$= \log_e 2 \tag{46}$$

which is unchanged from both the frequency-flat faded and the unfaded channels, roughly -1.59 dB [23]. The slope of the spectral efficiency per 3 dB of $\frac{E_b}{N_0}$ at $\frac{E_b}{N_0}_{\min}$, denoted S_0^{mmse}, is [23]

$$S_0^{\mathsf{mmse}} = \frac{2(\dot{\mathsf{C}}^{\mathsf{mmse}}(0))^2}{-\ddot{\mathsf{C}}^{\mathsf{mmse}}(0)} \log_e 2 \tag{47}$$

where $\dot{\mathsf{C}}^{\mathsf{mmse}}(\mathsf{snr})$ and $\ddot{\mathsf{C}}^{\mathsf{mmse}}(\mathsf{snr})$ are the first and second derivatives of $\mathsf{C}^{\mathsf{mmse}}(\mathsf{snr})$. In turn, the high-SNR slope of the MMSE spectral efficiency per 3 dB of $\frac{E_b}{N_0}$, denoted S_∞^{mmse}, equals [23]

$$S_\infty^{\mathsf{mmse}} = \lim_{\mathsf{snr}\to\infty} \frac{\mathsf{snr}\dot{\mathsf{C}}^{\mathsf{mmse}}(\mathsf{snr})}{\log_2 e}. \tag{48}$$

Invoking Properties 4.2–4.5 we have the following.

Proposition 4.1: Conditioned on the fading coefficients

$$S_0^{\mathsf{mmse}} = \frac{2\beta^2}{2\int_0^1 \left(\int_0^\beta \rho(x,y)dy\right)^2 dx + \int_0^\beta \left(\int_0^1 \rho(x,y)dx\right)^2 dy} \tag{49}$$

while

$$S_\infty^{\mathsf{mmse}} = \begin{cases} \beta\Pr\{\mathcal{Z}_Y(\mathsf{Y}) \neq 0\}, & \beta' < 1 \\ \frac{\beta}{2}\Pr\{\mathcal{Z}_Y(\mathsf{Y}) \neq 0\}, & \beta' = 1 \\ 0, & \beta' > 1. \end{cases} \tag{50}$$

Proof: In the Appendix, Part F.

Recall that, if the channel is not ergodic in frequency, the asymptotic performance measures still exhibit dependence on the channel realization. However, if there is temporal ergodicity, then the expected values of these asymptotic measures are meaningful quantities and we can thus define

$$\bar{\mathsf{C}}^{\mathsf{mmse}} = \mathbb{E}[\mathsf{C}^{\mathsf{mmse}}]$$
$$\bar{S}_\infty^{\mathsf{mmse}} = \mathbb{E}\,[S_\infty^{\mathsf{mmse}}]$$
$$\bar{S}_0^{\mathsf{mmse}} = \frac{2(\dot{\bar{\mathsf{C}}}^{\mathsf{mmse}}(0))^2}{-\ddot{\bar{\mathsf{C}}}^{\mathsf{mmse}}(0)} \log_e 2$$

where $\mathbb{E}[\cdot]$ denotes expectation with respect to the fading distribution.[6]

From Proposition 4.1, we have the following for channels that are ergodic in either frequency or time: if $\bar{Z}_X = 1$ (i.e., for almost every fading realization the fraction of subcarriers that are inactive is vanishingly small), then the high-SNR slope is unaffected by frequency-selective fading while the low-SNR slope is reduced with respect to the corresponding unfaded channel. This can be verified by noticing, using (12), that for channels nonergodic in frequency but temporally ergodic, $\rho(x,y)$ depends on the channel realization and consequently

$$\bar{S}_0^{\mathsf{mmse}} = \frac{2\beta}{2\beta\kappa(\sqrt{\bar{\mathsf{G}}_{\mathsf{H}}}) + \kappa(\sqrt{\bar{\mathsf{G}}_{\mathsf{A}}})} \tag{51}$$

where $\kappa(\sqrt{\bar{\mathsf{G}}_{\mathsf{H}}})$ and $\kappa(\sqrt{\bar{\mathsf{G}}_{\mathsf{A}}})$ indicate the respective kurtosis of the square roots of the average with respect to the fading distribution of the random variables[7]

$$\mathsf{G}_{\mathsf{H}} = \frac{1}{\beta}\int_0^\beta \rho(\mathsf{X},y)dy$$

and

$$\mathsf{G}_{\mathsf{A}} = \int_0^1 \rho(x,\mathsf{Y})dx$$

where X and Y are uniform on $[0,1]$ and $[0,\beta]$, respectively.[8] For channels ergodic in frequency, $\rho(x,y)$ does not depend on

[6]Henceforth, $\mathbb{E}[\cdot]$ and overbar (e.g., $\mathbb{E}[\xi]$ and $\bar{\xi}$) are used interchangeably to denote averaging with respect to the fading distribution. In the absence of such averaging indicators, the conditioning on the fading coefficients is implicit. In the case that the fading is ergodic in frequency, this distinction becomes, of course, immaterial. For distinctiveness, $E[\cdot]$ indicates expectation with respect to distributions other than the fading ensemble.

[7]Note that G_{H} and G_{A} have two different sources of randomness. One arises from the channel fading realization and the other one relates to the independent random variables X and Y uniform on $[0,1]$ and $[0,\beta]$, respectively.

[8]The kurtosis of a nonnegative random variable X, defined as

$$\kappa(X) = \mathrm{E}[X^4]/\mathrm{E}^2[X^2]$$

is a measure of the "peakedness" of its distribution and it is always greater than or equal to 1, with equality only if X is deterministic [23].

the channel realization and consequently neither do G_H and G_A. Thus,

$$S_0^{\mathsf{mmse}} = \frac{2\beta}{2\beta\kappa(\sqrt{\mathsf{G}_\mathsf{H}}) + \kappa(\sqrt{\mathsf{G}_\mathsf{A}})}. \tag{52}$$

In the absence of fading, i.e., with $\rho(x,y)$ constant with respect to x, $\kappa(\sqrt{\mathsf{G}_\mathsf{H}})$ equals 1. With frequency selectivity, in contrast, $\rho(x,y)$ varies with x and thus the kurtosis in (51) and (52) increase and the slope is diminished, from which we conclude that frequency-selective fading is detrimental at low SNR.

It is also interesting to study the effect of letting the number of users per subcarrier grow without bound.

Theorem 4.3: Conditioned on the fading coefficients

$$\mathsf{C}_\infty^{\mathsf{mmse}} = \lim_{\beta\to\infty} \mathsf{C}^{\mathsf{mmse}}\left(\frac{E_b}{N_0}\right)$$

is the solution to

$$\frac{E_b}{N_0}\int_0^1 \frac{\int_0^1 \tilde{\rho}(\tilde{x},\zeta)d\zeta}{1+\mathsf{C}_\infty^{\mathsf{mmse}}\frac{E_b}{N_0}\int_0^1 \tilde{\rho}(\tilde{x},\zeta)d\zeta}d\tilde{x} = \log_e 2 \tag{53}$$

where $\tilde{\rho}(\tilde{x},\tilde{y}) = \rho(\tilde{x},\beta\tilde{y})$ with $\rho(\cdot,\cdot)$ the channel profile function of $\frac{1}{\sqrt{Q}}\boldsymbol{HA}$ and $(\tilde{x},\tilde{y}) \in [0,1]^2$.

Proof: Defining $\tilde{\mu}(\tilde{y},\mathsf{snr}) = \mu(\beta\tilde{y},\mathsf{snr})$ with $\mu(\cdot,\cdot)$ given in (25)

$$\tilde{\mu}(\tilde{y},\mathsf{snr}) = \int_0^1 \frac{\tilde{\rho}(\tilde{x},\tilde{y})}{1+\mathsf{snr}\beta\int_0^1 \frac{\tilde{\rho}(\tilde{x},\zeta)}{1+\mathsf{snr}\tilde{\mu}(\zeta,\mathsf{snr})}d\zeta}d\tilde{x}. \tag{54}$$

Further, introducing $\tilde{\mu}_\infty(\tilde{y},\mathsf{snr}) = \lim_{\beta\to\infty}\tilde{\mu}(\tilde{y},\mathsf{snr})$ and using (19), we find

$$\tilde{\mu}_\infty(\tilde{y},\mathsf{snr}) = \int_0^1 \frac{\tilde{\rho}(\tilde{x},\tilde{y})}{1+\frac{E_b}{N_0}\mathsf{C}_\infty^{\mathsf{mmse}}\int_0^1 \tilde{\rho}(\tilde{x},\zeta)d\zeta}d\tilde{x}. \tag{55}$$

Letting $\beta\to\infty$ in (24) and invoking again (19), we obtain

$$\mathsf{C}_\infty^{\mathsf{mmse}}\frac{E_b}{N_0}\int_0^1 \tilde{\mu}_\infty(\tilde{y},\mathsf{snr})d\tilde{y} = \mathsf{C}_\infty^{\mathsf{mmse}}\log_e 2. \tag{56}$$

Combining (55) and (56), the claim is proved. □

Equation (53) has operation meaning for channels ergodic in frequency. In the case of channels nonergodic in frequency but temporally ergodic, Theorem 4.3 can be rewritten in terms of the more insightful measure $\bar{\mathsf{C}}_\infty^{\mathsf{mmse}}$ as follows:

$$\frac{E_b^t}{N_0}\mathbb{E}\left[\int_0^1 \frac{Q\int_0^1 \tilde{\rho}(\tilde{x},\zeta)d\zeta}{1+\bar{\mathsf{C}}_\infty^{\mathsf{mmse}}\frac{E_b^t}{N_0}Q\int_0^1 \tilde{\rho}(\tilde{x},\zeta)d\zeta}d\tilde{x}\right] = \log_e 2 \tag{57}$$

with $\frac{E_b^t}{N_0} = \frac{1}{Q}\frac{E_b}{N_0}$ the normalized transmitted energy per bit defined in (20).

Equations (53) and (57) lead, upon application of Jensen's inequality, to

$$\mathsf{C}_\infty^{\mathsf{mmse}} \le \log_2 e - \frac{1}{\frac{E_b}{N_0}} \text{ bits/s/Hz} \tag{58}$$

and

$$\bar{\mathsf{C}}_\infty^{\mathsf{mmse}} \le \log_2 e - \frac{1}{\bar{Q}\frac{E_b^t}{N_0}} \text{ bits/s/Hz} \tag{59}$$

where the upper bound is achieved by the MMSE spectral efficiency for $\beta\to\infty$ with either no fading or frequency-flat fading. For channels ergodic in frequency, Q equals its own average with respect to the fading distribution (i.e., $Q = \bar{Q}$) and consequently, $\frac{E_b^t}{N_0} = \frac{E_b}{N_0}/\bar{Q}$.

As in DS-CDMA [23], also for MC-CDMA we can observe that, with respect to the case of unfaded channel with $|A_k|^2 = 1$ for every k, flat fading increases the spectral efficiency in the region of high β because, at every instant, a certain proportion of interferers are faded and thus the number of *effective* interferers seen by the MMSE receiver is reduced. This interference population control effect of fading more than compensates for its deleterious effect on the desired user [23]. In particular, for $\beta\to\infty$, the MMSE spectral efficiencies with both no fading and frequency-flat fading coincide. Frequency selectivity, however, attenuates this interference population control and thus it diminishes the corresponding MMSE spectral efficiency for large β.

B. Downlink

As discussed in Section III-B, the downlink is a special case of the uplink where the subcarrier fading coefficients become common to all users, i.e., $H_k^i = H^i\ \forall\ k$. As a result of this commonality, the two-dimensional channel profile function of $\frac{1}{\sqrt{Q}}\boldsymbol{HA}$ can be expressed as

$$\rho(x,y) = \frac{1}{Q_xQ_y}\rho_{\boldsymbol{H}}(x)\rho_{\boldsymbol{A}}(y) \tag{60}$$

where $\rho_{\boldsymbol{H}}(\cdot)$ and $\rho_{\boldsymbol{A}}(\cdot)$ are the one-dimensional channel profile functions of $[|H^1|^2,\ldots,|H^N|^2]$ and $[|A_1|^2,\ldots,|A_K|^2]$, respectively, while $Q = Q_xQ_y$ as per (14). Furthermore, the one-dimensional channel profile function of kth column of $\frac{1}{\sqrt{Q}}\boldsymbol{HA}$ specializes to

$$\rho_k(x) = \frac{1}{Q_xQ_y}|A_k|^2\rho_{\boldsymbol{H}}(x). \tag{61}$$

Define independent random variables $|\mathsf{H}|^2$ and $|\mathsf{A}|^2$ whose distributions are given by those of $\frac{1}{Q_x}\rho_{\boldsymbol{H}}(\mathsf{X})$ and $\frac{1}{Q_y}\rho_{\boldsymbol{A}}(\mathsf{Y})$ with X and Y independent random variables uniform on $[0,1]$ and $[0,\beta]$, respectively. From (5)

$$\int_0^\beta \left(\frac{1}{Q_y}\rho_{\boldsymbol{A}}(y)\right)^k dy = \beta\mathrm{E}[(|\mathsf{A}|^2)^k] \tag{62}$$

$$\int_0^1 \left(\frac{1}{Q_x}\rho_{\boldsymbol{H}}(x)\right)^k dx = \mathrm{E}[(|\mathsf{H}|^2)^k]. \tag{63}$$

Note that $\mathrm{E}[|\mathsf{H}|^2] = \mathrm{E}[|\mathsf{A}|^2] = 1$. Applying (60) to (21) and (22), $v(x,\mathsf{snr})$ becomes the solution to (64) at the top of the following page, which, using (5), can be rewritten in terms of $|\mathsf{H}|^2$ and $|\mathsf{A}|^2$ as

$$\mathrm{E}[|\mathsf{H}|^2 v(|\mathsf{H}|^2,\mathsf{snr})] = \mathrm{E}\left[\frac{|\mathsf{H}|^2}{1+\mathsf{snr}|\mathsf{H}|^2\beta E\left[\frac{|\mathsf{A}|^2}{1+\mathsf{snr}|\mathsf{A}|^2\mathrm{E}[|\mathsf{H}|^2 v(|\mathsf{H}|^2,\mathsf{snr})]}\right]}\right]. \tag{65}$$

Finally, invoking

$$\int_0^1 \rho_k(x)dx = \frac{|A_k|^2}{Q_y}\mathrm{E}[|\mathsf{H}|^2] = \frac{|A_k|^2}{Q_y} \tag{66}$$

we can put forth the following.

$$\int_0^1 v(x,\mathsf{snr})\rho_{\boldsymbol{H}}(x)dx = \int_0^1 \frac{\rho_{\boldsymbol{H}}(x)}{1+\mathsf{snr}\frac{\rho_{\boldsymbol{H}}(x)}{Q_x}\int_0^\beta \frac{\frac{\rho_{\boldsymbol{A}}(y)}{Q_y}}{1+\mathsf{snr}\frac{\rho_{\boldsymbol{A}}(y)}{Q_y}\int_0^1 v(w,\mathsf{snr})\frac{\rho_{\boldsymbol{H}}(w)}{Q_x}dw}dy}dx \tag{64}$$

Corollary 4.1: Conditioned on the fading coefficients, the MMSE multiuser efficiency of every user, $\eta(\mathsf{snr})$, converges almost surely to the solution of

$$\eta = \mathrm{E}\left[\frac{|\mathsf{H}|^2}{1+\beta|\mathsf{H}|^2\mathrm{E}\left[\frac{\mathsf{snr}|\mathsf{A}|^2}{1+\mathsf{snr}\eta|\mathsf{A}|^2}\right]}\right]. \tag{67}$$

Recall that, with frequency ergodicity, (67) also provides the ergodic MMSE multiuser efficiency. The same observation holds for the remaining results.

The independence of the MMSE multiuser efficiency on the user index in the above theorem is a result of the commonality in the fading. Notice that, from (60)

$$\begin{aligned} Z_X &= \int_0^1 1\left\{\int_0^\beta \rho(x,y)dy \neq 0\right\}dx \\ &= \int_0^1 1\left\{\frac{1}{Q_x}\rho_{\boldsymbol{H}}(x)\neq 0\right\}dx \\ &= \Pr\left\{\frac{1}{Q_x}\rho_{\boldsymbol{H}}(\mathsf{X})\neq 0\right\} \\ &= \Pr\left\{|\mathsf{H}|^2\neq 0\right\}. \end{aligned} \tag{68}$$

Since Z_X turns out to be the probability that the random variable $|\mathsf{H}|^2$ is strictly positive, in the following we shall denote $\Pr\{|\mathsf{H}|^2\neq 0\}$ as $|\mathsf{H}|^+$. An analogous consideration can be made for Z_Y, i.e.,

$$\begin{aligned} Z_Y &= \int_0^\beta 1\left\{\int_0^1 \rho(x,y)dx \neq 0\right\}dy \\ &= \beta\Pr\left\{|\mathsf{A}|^2\neq 0\right\} \\ &= \beta|\mathsf{A}|^+. \end{aligned} \tag{69}$$

Recalling (38), the effective load can be seen to equal (for a given fading realization)

$$\beta' = \beta\frac{|\mathsf{A}|^+}{|\mathsf{H}|^+} \tag{70}$$

consistent with the fact that $K|\mathsf{A}|^+$ is roughly the number of users actively transmitting while $N|\mathsf{H}|^+$ is essentially the number of active subcarriers.

From Corollary 4.1 we observe, as in the uplink, that if the channel is ergodic in frequency then frequency-selective fading reduces the MMSE multiuser efficiency with respect to the case of no fading. In fact, (67) can be rewritten as

$$\eta\beta\mathrm{E}\left[\frac{\mathsf{snr}|\mathsf{A}|^2}{1+\mathsf{snr}\eta|\mathsf{A}|^2}\right] = 1-\mathrm{E}\left[\frac{1}{1+\beta|\mathsf{H}|^2\mathrm{E}\left[\frac{\mathsf{snr}|\mathsf{A}|^2}{1+\mathsf{snr}\eta|\mathsf{A}|^2}\right]}\right] \tag{71}$$

from which, applying Jensen's inequality

$$\eta \leq \frac{1}{1+\beta\mathrm{E}\left[\frac{\mathsf{snr}|\mathsf{A}|^2}{1+\mathsf{snr}\eta|\mathsf{A}|^2}\right]} \tag{72}$$

where strict equality yields the MMSE multiuser efficiency for an unfaded channel [26].

Next, we review the properties of $\eta(\mathsf{snr})$. Since they can be seen as special cases of the corresponding properties for the uplink, we omit the proofs.

Property 4.6:

$$\begin{aligned} \eta(\mathsf{snr}) = 1 &- \frac{\beta\mathrm{E}[(|\mathsf{H}|^2)^2]\mathsf{snr}}{(\mathrm{E}[|\mathsf{H}|^2])^2} \\ &+ \left(\frac{\beta^2\mathrm{E}[(|\mathsf{H}|^2)^3]}{(\mathrm{E}[|\mathsf{H}|^2])^3} + \frac{\beta\mathrm{E}[(|\mathsf{H}|^2)^2]\mathrm{E}[(|\mathsf{A}|^2)^2]}{(\mathrm{E}[|\mathsf{H}|^2])^2(\mathrm{E}[|\mathsf{A}|^2])^2}\right)\mathsf{snr}^2 \\ &+ o(\mathsf{snr}^2). \end{aligned} \tag{73}$$

Property 4.7:

$$\lim_{\mathsf{snr}\to\infty}\eta(\mathsf{snr}) = \begin{cases}\eta_0>0, & \beta'<1\\ 0, & \beta'\geq 1\end{cases} \tag{74}$$

where η_0 is the positive solution to

$$\mathrm{E}\left[\frac{|\mathsf{H}|^2}{\eta_0+\beta|\mathsf{A}|^+|\mathsf{H}|^2}\right] = 1. \tag{75}$$

Property 4.8:

$$\lim_{\mathsf{snr}\to\infty}\mathsf{snr}\eta(\mathsf{snr}) = \begin{cases}\infty, & \beta'\leq 1\\ \alpha, & \beta'>1\end{cases} \tag{76}$$

where α is the solution to

$$\frac{\beta}{|\mathsf{H}|^+}\mathrm{E}\left[\frac{\alpha|\mathsf{A}|^2}{1+\alpha|\mathsf{A}|^2}\right] = 1. \tag{77}$$

Property 4.9:

$$\lim_{\mathsf{snr}\to\infty}\frac{\mathsf{snr}\dot{\eta}(\mathsf{snr})}{\eta(\mathsf{snr})} = \begin{cases}0, & \beta'<1\\ -\frac{1}{2}, & \beta'=1\\ -1, & \beta'>1.\end{cases} \tag{78}$$

From the asymptotic MMSE multiuser efficiency, we can now characterize the corresponding asymptotic spectral efficiency.

Corollary 4.2: Conditioned on the fading coefficients, the linear MMSE spectral efficiency converges to

$$\mathsf{C}^{\mathsf{mmse}} = \beta\mathrm{E}\left[\log_2\left(1+\mathsf{snr}\eta|\mathsf{A}|^2\right)\right] \tag{79}$$

where η is the MMSE multiuser efficiency satisfying (67).

The reduction of η by subcarrier fading also decreases the MMSE spectral efficiency with respect to the corresponding unfaded channel.

The low- and high-SNR performance measures derived for the uplink can be easily specialized as follows. The $\frac{E_b}{N_0}_{\min}$ is unaffected by the fading. For S_0, using Property 4.6

$$\dot{\mathsf{C}}^{\mathsf{mmse}}(0) = \frac{\beta}{\log_e 2} \tag{80}$$

$$\begin{aligned} \ddot{\mathsf{C}}^{\mathsf{mmse}}(0) &= -\frac{\beta}{\log_e 2} \\ &\quad\cdot\left(\frac{2\beta\mathrm{E}[(|\mathsf{H}|^2)^2]}{\mathrm{E}[|\mathsf{H}|^2]} + \frac{\mathrm{E}[(|\mathsf{A}|^2)^2]}{\mathrm{E}[|\mathsf{A}|^2]}\right) \end{aligned} \tag{81}$$

$$= -\frac{\beta}{\log_e 2}\left[2\beta\kappa(|\mathsf{H}|)+\kappa(|\mathsf{A}|)\right] \tag{82}$$

where in (82) we have used the fact that $\mathrm{E}[|\mathsf{H}|^2] = \mathrm{E}[|\mathsf{A}|^2] = 1$ and where $\kappa(|\mathsf{H}|)$ and $\kappa(|\mathsf{A}|)$ indicate the kurtosis of the square roots of the random variables $|\mathsf{H}|^2$ and $|\mathsf{A}|^2$, respectively. Hence, conditioned on the fading coefficients, from (47)

$$S_0^{\mathsf{mmse}} = \frac{2\beta}{2\beta\kappa(|\mathsf{H}|) + \kappa(|\mathsf{A}|)}. \tag{83}$$

With respect to an unfaded channel, for channels ergodic in frequency, the low-SNR slope is reduced by the frequency-selective fading. For channels not ergodic in frequency but temporally ergodic, using $\mathrm{E}[|\mathsf{H}|^2] = 1$ and $\kappa(|\mathsf{H}|) = \mathrm{E}[(|\mathsf{H}|^2)^2]$

$$\bar{S}_0^{\mathsf{mmse}} = \frac{2\beta}{2\beta\mathbb{E}\left[\kappa(|\mathsf{H}|)\right] + \kappa(|\mathsf{A}|)} \tag{84}$$

where again $\mathbb{E}[\cdot]$ denotes expectation with respect to the subcarrier fading distribution. From (84), we observe that with respect to the unfaded channel the slope is reduced.

In turn, from (48) and Properties 4.7–4.9, the high-SNR slope is

$$S_\infty^{\mathsf{mmse}} = \begin{cases} \beta|\mathsf{A}|^+, & \beta' < 1 \\ \frac{1}{2}\beta|\mathsf{A}|^+, & \beta' = 1 \\ 0, & \beta' > 1 \end{cases} \tag{85}$$

which is not affected by fading if $|\mathsf{H}|^+ = 1$. Thus, following the same considerations as those of Section IV-A, fading does not degrade the high-SNR slope if $\mathbb{E}[|\mathsf{H}|^+] = 1$ whenever the channel is ergodic in either frequency or time. It is also evidenced by (85) that the MMSE spectral efficiency grows without bound as $\frac{E_b}{N_0} \to \infty$ if $\beta' \leq 1$. If $\beta' > 1$, in contrast, Property 4.8 evidences that the MMSE receiver is interference limited and the spectral efficiency converges, as $\frac{E_b}{N_0} \to \infty$, to

$$\lim_{\mathsf{snr}\to\infty} \mathsf{C}^{\mathsf{mmse}} = \beta \mathrm{E}\left[\log_2\left(1 + \alpha|\mathsf{A}|^2\right)\right] \tag{86}$$

where α satisfies (77). For unfaded channels[9]

$$\alpha^{\mathrm{uf}} = \lim_{\mathsf{snr}\to\infty} \mathsf{snr}\,\eta^{\mathrm{uf}}(\mathsf{snr}) \tag{87}$$

satisfies

$$\beta \mathrm{E}\left[\frac{\alpha^{\mathrm{uf}}|\mathsf{A}|^2}{1 + \alpha^{\mathrm{uf}}|\mathsf{A}|^2}\right] = 1 \tag{88}$$

if $\beta|\mathsf{A}|^+ > 1$. Comparing (88) with (77), we observe an interesting phenomenon in channels that are ergodic in frequency: if $\beta|\mathsf{A}|^+ > |\mathsf{H}|^+$ and $|\mathsf{H}|^+ = 1$, then the spectral efficiency gap between frequency-selective faded and unfaded channels is bridged as $\frac{E_b}{N_0} \to \infty$. However, if $|\mathsf{H}|^+ < 1$, then the spectral efficiency with frequency-selective fading is strictly smaller than that of the corresponding unfaded channel even as $\frac{E_b}{N_0} \to \infty$. The cause of this nonzero loss is that, when some subcarriers are inactive, the energy allocated to them is wasted.

[9]The superscript uf indicates that a quantity is evaluated for the corresponding unfaded channel, i.e., with $H_k^i = 1\ \forall\, i, k$ but retaining the same set of A_k's present in the fading channel.

Particularizing Theorem 4.3 to the downlink, we obtain the following theorem.

Theorem 4.4: Conditioned on the fading coefficients

$$\mathsf{C}_\infty^{\mathsf{mmse}} = \lim_{\beta\to\infty} \mathsf{C}^{\mathsf{mmse}}\left(\frac{E_b}{N_0}\right) \tag{89}$$

is the solution to

$$\mathrm{E}\left[\frac{\frac{E_b}{N_0}|\mathsf{H}|^2}{1 + \mathsf{C}_\infty^{\mathsf{mmse}}\frac{E_b}{N_0}|\mathsf{H}|^2}\right] = \log_e 2. \tag{90}$$

We note that (90) can also be written as

$$1 - \mathsf{C}_\infty^{\mathsf{mmse}} \log_e 2 = \mathrm{E}\left[\frac{1}{1 + \mathsf{C}_\infty^{\mathsf{mmse}}\frac{E_b}{N_0}|\mathsf{H}|^2}\right] \tag{91}$$

which leads, upon application of Jensen's inequality, to

$$\mathsf{C}_\infty^{\mathsf{mmse}} \leq \log_2 e - \frac{1}{Q_y Q_x \frac{E_b^t}{N_0}} \text{ bits/s/Hz} \tag{92}$$

whose right-hand side is the MMSE spectral efficiency for $\beta \to \infty$ with either no fading or frequency-flat fading at a received normalized energy per bit equal to $(1/Q_yQ_x)\frac{E_b^t}{N_0}$. Note that, for channels ergodic in frequency, $Q_x = \bar{Q}_x = 1$. Inequality (92) is mirrored, for channels nonergodic in frequency but temporally ergodic, by

$$\bar{\mathsf{C}}_\infty^{\mathsf{mmse}} \leq \log_2 e - \frac{1}{Q_y \bar{Q}_x \frac{E_b^t}{N_0}} \text{ bits/s/Hz}. \tag{93}$$

Hence, frequency selectivity in the fading reduces the MMSE spectral efficiency even as $\beta \to \infty$. This loss is similar to the loss associated with $\mathbb{E}[|\mathsf{H}|^+] < 1$, namely, frequency selectivity reduces the number of effective available subcarriers.

Figs. 1 and 2 show, for $\beta = 0.6$ and $\beta = 2.5$, respectively, the MMSE spectral efficiency versus $\frac{E_b}{N_0}$ for both a frequency-selective faded channel and its unfaded counterpart. An exponential distribution was used for the asymptotic spectrum of $\boldsymbol{A}\boldsymbol{A}^\dagger$ while the subcarrier fading coefficients are modeled as independent Rayleigh random variables with variance $\mathbb{E}[|H^i|^2] = 1$ (from which, because of ergodicity in frequency, $\kappa(|\mathsf{H}|) = 2$). From the figures, it can be appreciated that $\frac{E_b}{N_0\,\mathrm{min}}$ and the slope at high SNR are unaffected by multicarrier fading while the slope at low SNR is reduced. We also observe, from Fig. 2, that the MMSE spectral efficiency is bounded for $\beta' > 1$, and that the loss due to subcarrier fading vanishes as $\frac{E_b}{N_0} \to \infty$ if $\beta|\mathsf{A}|^+ > |\mathsf{H}|^+ = 1$.

Fig. 3 compares the MMSE spectral efficiency (as a function of β) with both frequency-selective fading and no fading for $\frac{E_b}{N_0} = 10$ dB.

Interestingly, the factorization of the channel profile function in (60), which results in the simplified downlink expressions, also takes place—asymptotically only—in the statistically symmetric uplink (where, recall, the users are statistically equivalent and the fading is ergodic in frequency). In such conditions, $\boldsymbol{H}$ is such that the empirical distribution of the subcarrier fading coefficients for the kth user, $\left[H_k^1, \ldots, H_k^N\right]$, converges almost surely to a nonrandom limit, common to all users and subcarriers, that coincides with the marginal distribution of H_k^i. From these considerations, it is proved in [29, Theorem 2.49] that the

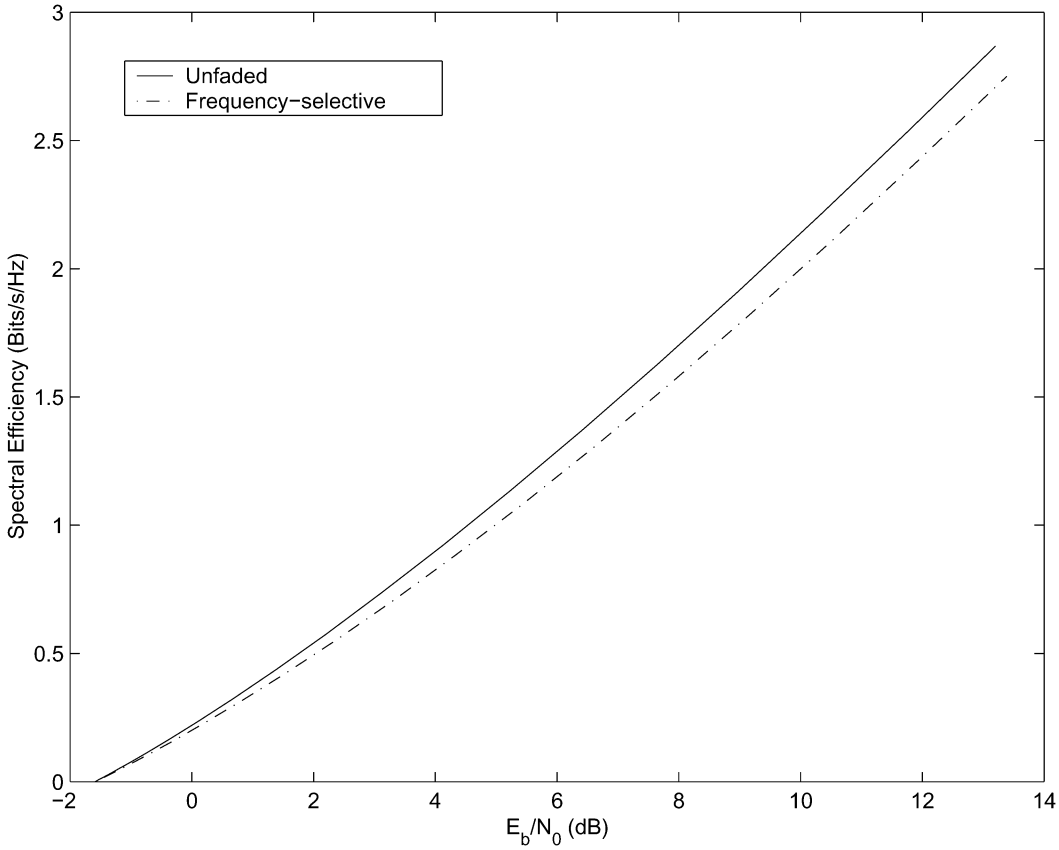

Fig. 1. MMSE spectral efficiency for $\beta = 0.6$.

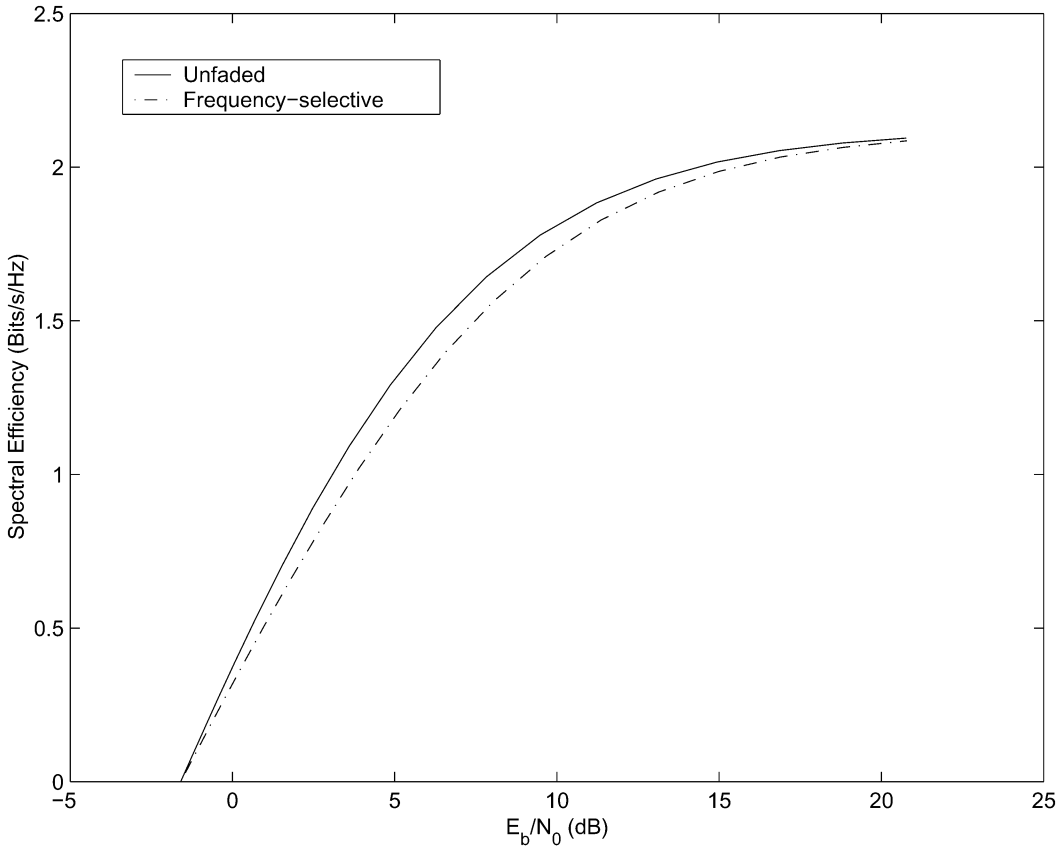

Fig. 2. MMSE spectral efficiency for $\beta = 2.5$.

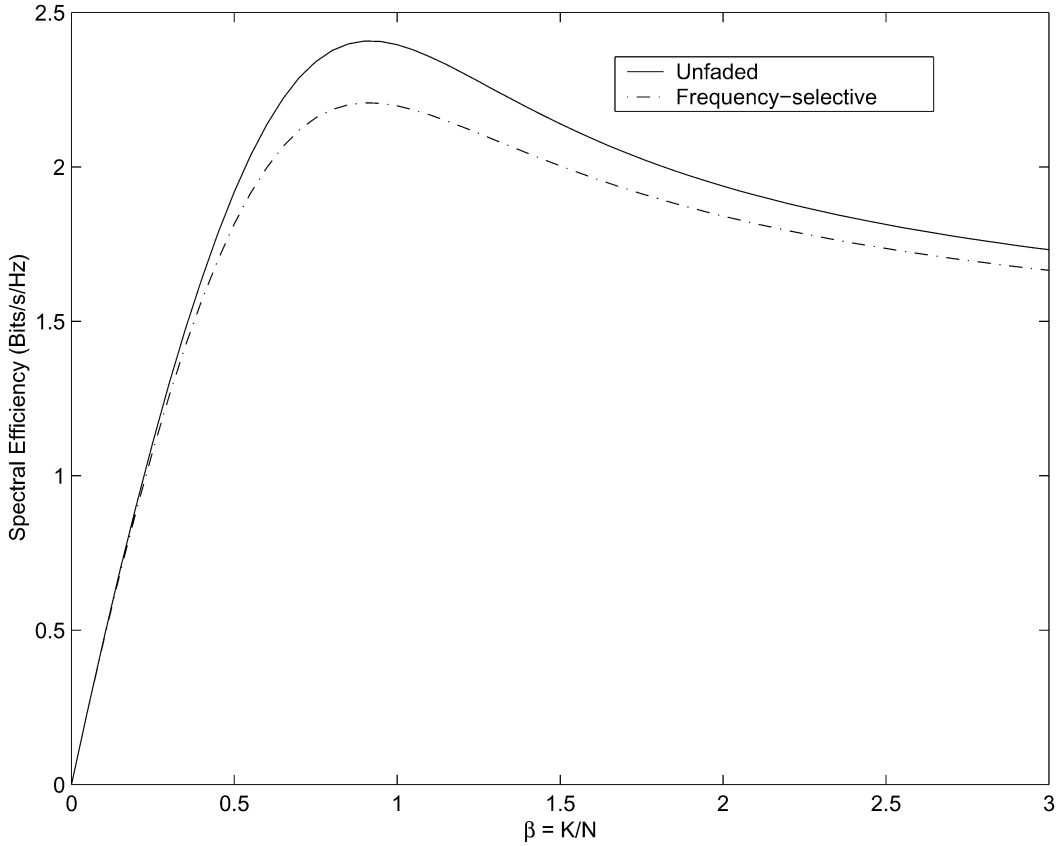

Fig. 3. MMSE spectral efficiency for $\frac{E_b}{N_0} = 10$ dB.

empirical distribution of the squared singular values of $\boldsymbol{H} \circ \boldsymbol{S}$ converges almost surely to the Marcenko–Pastur law with parameter β [29, eq. (1.12)]. This law gives the asymptotic empirical distribution of the squared singular values of an $N \times K$ random matrix whose entries are i.i.d. with variance $1/N$. Following the same steps of [29, Theorem 2.49], it can be proved that the spectrum of $\tilde{\boldsymbol{S}}\tilde{\boldsymbol{S}}^{\dagger}$ converges almost surely to a nonrandom limit whose Stieltjes transform is given by (6) and (7) with $\rho_{\boldsymbol{D}}(x, y) = \rho_{\boldsymbol{A}}(y)$ where there is no dependence on x and $\rho_{\boldsymbol{A}}(\cdot)$ denotes the one-dimensional channel profile function of $[|A_1|^2, \ldots, |A_k|^2]$. Hence, the results developed in this section can be reformulated for the statistically symmetric uplink by just letting $|\mathsf{H}| = 1$ while the distribution of $|\mathsf{A}|^2$ is still given by the empirical eigenvalue distribution of $\frac{1}{Q_y}\boldsymbol{A}\boldsymbol{A}^{\dagger}$. Specifically we have the following.

Theorem 4.5: Given an uplink channel as in (9), ergodic in frequency and having statistically symmetric subcarrier fading across the users, the empirical eigenvalue distribution of $\tilde{\boldsymbol{S}}\tilde{\boldsymbol{S}}^{\dagger}$ converges almost surely to a nonrandom distribution function whose Stieltjes transform satisfies

$$\mathcal{S}_{\tilde{\boldsymbol{S}}}(z) = \frac{1}{1 + z\mathrm{E}\left[\frac{|\mathsf{A}|^2}{1+z|\mathsf{A}|^2\mathcal{S}_{\tilde{\boldsymbol{S}}}(z)}\right]}. \tag{94}$$

Consequently, the performance measures for the statistically symmetric and frequency ergodic uplink admit a simpler formulation that coincides with that for the corresponding unfaded channels.

V. Optimum Receiver

Let us now consider jointly optimum (nonlinear) processing. For a given matrix of received spreading sequences $\tilde{\boldsymbol{S}}$, the capacity of an optimum receiver is [34]

$$\mathsf{C}^{\mathsf{opt}} = \frac{1}{N}\log_2 \det\left(\boldsymbol{I} + \frac{\mathsf{snr}}{Q}\tilde{\boldsymbol{S}}\tilde{\boldsymbol{S}}^{\dagger}\right). \tag{95}$$

A. Uplink

The next theorem is very relevant from the viewpoint of receiver design. The additional capacity achieved by going from linear to nonlinear processing for DS-CDMA and MC-CDMA channels subject to frequency-flat fading was found in [23]. As in [23], we find here that the capacity gain attained by optimum nonlinear processing depends only on the linear uncoded performance measure $\mu(y', \mathsf{snr})$, which is proportional to the output SINR of the y'th user with y' denoting the normalized (by N) user index.

As in Section IV-A, $\rho(x, y)$ and $\rho_k(x)$ with $x \in [0, 1]$ and $y \in [0, \beta]$ denote the two-dimensional and, for a given k, the one-dimensional channel profile of $\frac{1}{\sqrt{Q}}\boldsymbol{H}\boldsymbol{A}$.

Theorem 5.1: Conditioned on the fading coefficients, as $K, N \to \infty$ with $\frac{K}{N} \to \beta$, the optimum capacity can be expressed in terms of the MMSE spectral efficiency as

$$\mathsf{C}^{\mathsf{opt}} = \mathsf{C}^{\mathsf{mmse}} - \log_2 e \cdot \int_0^{\beta} \mu(y', \mathsf{snr})\pi(y', \mathsf{snr})dy' + \int_0^1 \log_2\left(1 + \int_0^{\beta} \rho(x, y')\pi(y', \mathsf{snr})dy'\right)dx \tag{96}$$

where

$$\pi(y', \mathsf{snr}) = \frac{\mathsf{snr}}{1 + \mathsf{snr}\mu(y', \mathsf{snr})} \tag{97}$$

and $\mu(\cdot, \mathsf{snr})$ is the solution to (25).

Proof: In the Appendix, Part E.

In channels ergodic in frequency, once again, the above conditioned result coincides with its unconditioned (ergodic) counterpart.

From Theorem 4.2, in conjunction with the well-known fact that successive cancellation with MMSE multiuser detection that ignores previously decoded users achieves the optimum capacity given perfect cancellation [17], [31], [22], the following corollary ensues.

Corollary 5.1: Conditioned on the fading coefficients, the optimum capacity converges almost surely to

$$\mathsf{C}^{\mathsf{opt}} = \int_0^\beta \log_2 \left(1 + \mathsf{snr}\nu(y', \mathsf{snr})\right) dy' \tag{98}$$

where $\nu(\cdot, \mathsf{snr})$ is the solution to

$$\nu(y', \mathsf{snr}) = \int_0^1 \frac{\rho(x, y')dx}{1 + \mathsf{snr}\int_0^{y'} \frac{\rho(x,y)}{1+\mathsf{snr}\nu(y,\mathsf{snr})} dy}. \tag{99}$$

From (95) and (10)

$$\begin{aligned} \dot{\mathsf{C}}^{\mathsf{opt}}(0) &= \frac{1}{\log_e 2} \lim_{N\to\infty} \frac{1}{QN} \mathrm{Tr}\{\tilde{\boldsymbol{S}}\tilde{\boldsymbol{S}}^\dagger\} \\ &\overset{\text{a.s.}}{=} \frac{1}{\log_e 2} \frac{\beta}{Q} \lim_{K\to\infty} \frac{\|\boldsymbol{H}\boldsymbol{A}\|^2}{KN} \\ &= \frac{\beta}{\log_e 2} \end{aligned} \tag{100}$$

thus, the minimum received normalized energy per bit required for reliable communication is

$$\begin{aligned} \frac{E_b}{N_0}_{\min} &= \lim_{\mathsf{snr}\to 0} \frac{\beta \mathsf{snr}}{\mathsf{C}^{\mathsf{opt}}(\mathsf{snr})} \\ &= \frac{\beta}{\dot{\mathsf{C}}^{\mathsf{opt}}(0)} \\ &= \log_e 2. \end{aligned} \tag{101}$$

The slope of $\mathsf{C}^{\mathsf{opt}}$ in bits/s/Hz per 3 dB at $\frac{E_b}{N_0}_{\min}$ is [23]

$$S_0^{\mathsf{opt}} = \frac{2(\dot{\mathsf{C}}^{\mathsf{opt}}(0))^2}{-\ddot{\mathsf{C}}^{\mathsf{opt}}(0)} \log_e 2 \tag{102}$$

while the slope at high $\frac{E_b}{N_0}$ in bits/s/Hz per 3 dB is

$$S_\infty^{\mathsf{opt}} = \lim_{\mathsf{snr}\to\infty} \frac{\mathsf{snr}\dot{\mathsf{C}}^{\mathsf{opt}}(\mathsf{snr})}{\log_2 e}. \tag{103}$$

From [14], the second moment of $\frac{1}{Q}\tilde{\boldsymbol{S}}\tilde{\boldsymbol{S}}^\dagger$ conditioned on the fading converges almost surely to

$$\begin{aligned} \frac{1}{N}\left\|\frac{1}{Q}\tilde{\boldsymbol{S}}\tilde{\boldsymbol{S}}^\dagger\right\|^2 &\to \lim_{N\to\infty} \frac{1}{N}\mathrm{Tr}\left\{\left(\frac{1}{Q}\boldsymbol{H}\boldsymbol{A}\boldsymbol{A}^\dagger\boldsymbol{H}^\dagger\right)^2\right\} \\ &= \int_0^1 \left(\int_0^\beta \rho(x,y)dy\right)^2 dx \\ &\quad + \int_0^\beta \left(\int_0^1 \rho(x,y)dx\right)^2 dy \end{aligned} \tag{104}$$

from which we get the following.

Proposition 5.1: Conditioned on the fading coefficients

$$S_0^{\mathsf{opt}} = \frac{2\beta^2}{\int_0^1 \left(\int_0^\beta \rho(x,y)dy\right)^2 dx + \int_0^\beta \left(\int_0^1 \rho(x,y)dx\right)^2 dy} \tag{105}$$

and

$$S_\infty^{\mathsf{opt}} = \min\{\beta \Pr\{\mathcal{Z}_Y(\mathsf{Y}) \neq 0\}, \Pr\{\mathcal{Z}_X(\mathsf{X}) \neq 0\}\} \tag{106}$$

with $\mathcal{Z}_X(\cdot)$ and $\mathcal{Z}_Y(\cdot)$ defined in (37) and with X and Y uniform on $[0,1]$ and $[0,\beta]$, respectively.

Proof: In the Appendix, Part G.

The counterparts of (105) and (106) in the case of channels nonergodic in frequency but temporally ergodic are as in (107) at the bottom of the page, and

$$\bar{S}_\infty^{\mathsf{opt}} = \min\{\beta \mathbb{E}[\Pr\{\mathcal{Z}_Y(\mathsf{Y}) \neq 0\}], \mathbb{E}[\Pr\{\mathcal{Z}_X(\mathsf{X}) \neq 0\}]\} \tag{108}$$

from which, in conjunction with (105) and (106), it follows—as for the MMSE receiver—that if the channel is ergodic in either frequency or time, frequency-selective fading reduces the low-SNR slope with respect to the corresponding unfaded channel while the high-SNR slope is affected only if there is a nonvanishing fraction of subcarriers that are inactive for every user in a set of channel realizations with nonzero measure. Equations (107) and (108) can be derived following the same steps used to derive Proposition 5.1 but with $\bar{\mathsf{C}}^{\mathsf{opt}}$ rather than $\mathsf{C}^{\mathsf{opt}}$ as starting point.

From (198) given in the Appendix, Part E

$$\dot{\mathsf{C}}^{\mathsf{opt}}(\mathsf{snr}) = 1 - \int_0^1 \frac{1}{1 + \mathsf{snr}\int_0^\beta \frac{\rho(x,y)}{1+\mathsf{snr}\mu(y,\mathsf{snr})} dy} dx \tag{109}$$

with

$$\begin{aligned} &\int_0^\beta \frac{\mathsf{snr}\mu(y,\mathsf{snr})}{1 + \mathsf{snr}\mu(y,\mathsf{snr})} dy \\ &\qquad = 1 - \int_0^1 \frac{1}{1 + \mathsf{snr}\int_0^\beta \frac{\rho(x,y)}{1+\mathsf{snr}\mu(y,\mathsf{snr})} dy} dx \end{aligned} \tag{110}$$

$$\bar{S}_0^{\mathsf{opt}} = \frac{2\beta^2}{\int_0^1 \mathbb{E}\left[\left(\int_0^\beta \rho(x,y)dy\right)^2\right] dx + \int_0^\beta \mathbb{E}\left[\left(\int_0^1 \rho(x,y)dx\right)^2\right] dy} \tag{107}$$

from which the following ensues: with frequency-selective fading, $\dot{\bar{\mathsf{C}}}^{\mathsf{opt}}(\mathsf{snr})$ is upper-bounded by the value it takes with no fading and, consequently, so is the ergodic capacity $\bar{\mathsf{C}}^{\mathsf{opt}}(\mathsf{snr})$.

For $\beta \to \infty$, we derive the following result.

Theorem 5.2: Conditioned on the fading, the optimum capacity converges as $\beta \to \infty$ to the solution of

$$\mathsf{C}_\infty^{\mathsf{opt}} = \int_0^1 \log_2\left(1 + \mathsf{C}_\infty^{\mathsf{opt}} \frac{E_b}{N_0} \int_0^1 \tilde{\rho}(\tilde{x},\tilde{y}) d\tilde{y}\right) d\tilde{x} \tag{111}$$

with $\tilde{\rho}(\cdot,\cdot)$ defined as in Theorem 4.3.

Proof: Applying (19), (96) can be rewritten in terms of $\tilde{\rho}(\tilde{x},\tilde{y})$ as

$$\begin{aligned}\mathsf{C}^{\mathsf{opt}} &= \mathsf{C}^{\mathsf{mmse}} - \beta\mathsf{snr}\int_0^1 \frac{\tilde{\mu}(\tilde{y},\mathsf{snr})}{1+\mathsf{snr}\tilde{\mu}(\tilde{y},\mathsf{snr})} d\tilde{y} \log_2 e \\ &\quad + \int_0^1 \log_2\left(1+\beta\mathsf{snr}\int_0^1 \frac{\tilde{\rho}(\tilde{x},\zeta)}{1+\mathsf{snr}\tilde{\mu}(\zeta,\mathsf{snr})} d\zeta\right) d\tilde{x} \qquad (112)\\ &= \mathsf{C}^{\mathsf{mmse}} - \log_2 e \frac{E_b}{N_0}\mathsf{C}^{\mathsf{opt}} \int_0^1 \frac{\tilde{\mu}(\tilde{y},\mathsf{snr})}{1+\frac{E_b}{N_0}\frac{\mathsf{C}^{\mathsf{opt}}}{\beta}\tilde{\mu}(\tilde{y},\mathsf{snr})} d\tilde{y} \\ &\quad + \int_0^1 \log_2\left(1+\frac{E_b}{N_0}\mathsf{C}^{\mathsf{opt}}\int_0^1 \frac{\tilde{\rho}(\tilde{x},\tilde{y})}{1+\frac{E_b}{N_0}\frac{\mathsf{C}^{\mathsf{opt}}}{\beta}\tilde{\mu}(\tilde{y},\mathsf{snr})} d\tilde{y}\right) d\tilde{x} \qquad (113)\end{aligned}$$

where $\tilde{\mu}(\cdot,\mathsf{snr})$ is the solution to (54). Applying (55) to (113), (111) follows immediately. □

In order to draw some engineering insight on the impact of frequency selectivity with respect to the corresponding unfaded and frequency-flat scenarios, let us focus on regime of high-load factor. Following Theorem 5.2, we obtain the counterpart of (111) for temporally ergodic channels in terms of normalized transmitted energy per bit as

$$\bar{\mathsf{C}}_\infty^{\mathsf{opt}} = \int_0^1 \mathbb{E}\left[\log_2\left(1+\bar{\mathsf{C}}_\infty^{\mathsf{opt}}\frac{E_b^t}{N_0} Q \int_0^1 \tilde{\rho}(\tilde{x},\tilde{y}) d\tilde{y}\right)\right] d\tilde{x} \tag{114}$$

which, applying Jensen's inequality, yields

$$\bar{\mathsf{C}}_\infty^{\mathsf{opt}} \le \log_2\left(1+\bar{\mathsf{C}}_\infty^{\mathsf{opt}}\frac{E_b^t}{N_0}\bar{Q}\right) \tag{115}$$

whose right-hand side maps onto the single-user unfaded channel. It is verified from Theorem 5.2, as proved in [23], that in the case of unfaded and frequency-flat faded channels, the optimum capacity achieves the above upper bound for $\beta \to \infty$ and the inequality becomes a strict equality. Therefore, in contrast with the flat-fading case, where as $\beta \to \infty$ the channel can be used as efficiently as if all of the power was concentrated in one user and the effect of fading had vanished, in the frequency-selective case the optimum receiver is not able to wipe out the entire fading penalty. This behavior is, of course, upheld when the channel is not temporally ergodic but it is ergodic in frequency.

B. Downlink

Using the downlink factorization of $\rho(\cdot,\cdot)$ and (62)–(67), Theorem 5.1 can be reformulated for the downlink. From (96) and (97)

$$\begin{aligned}\int_0^\beta \mu(y',\mathsf{snr})\pi(y',\mathsf{snr})dy' &= \frac{\eta}{Q_y}\int_0^\beta \rho_{\boldsymbol{A}}(y')\pi(y',\mathsf{snr})dy \\ &= \eta\int_0^\beta \frac{\mathsf{snr}\frac{\rho_{\boldsymbol{A}}(y')}{Q_y}}{1+\mathsf{snr}\eta\frac{\rho_{\boldsymbol{A}}}{Q_y}(y')} \\ &= \eta\mathrm{E}\left[\frac{\mathsf{snr}|\mathsf{A}|^2}{1+\mathsf{snr}\eta|\mathsf{A}|^2}\right] \qquad (116)\end{aligned}$$

with η satisfying (67) while $|\mathsf{H}|^2$ and $|\mathsf{A}|^2$ indicate independent random variables defined as in Section IV-B. Then, the expression of the optimum downlink capacity in terms of the MMSE spectral efficiency is as follows.

Corollary 5.2: Conditioned on the subcarrier fading coefficients, the optimum downlink capacity converges almost surely to

$$\begin{aligned}\mathsf{C}^{\mathsf{opt}} = \mathsf{C}^{\mathsf{mmse}} &+ \mathrm{E}\left[\log_2\left(1+\beta|\mathsf{H}|^2\mathrm{E}\left[\frac{\mathsf{snr}|\mathsf{A}|^2}{1+\mathsf{snr}\eta|\mathsf{A}|^2}\right]\right)\right] \\ &-\beta\mathrm{E}\left[\frac{\mathsf{snr}\eta|\mathsf{A}|^2}{1+\mathsf{snr}\eta|\mathsf{A}|^2}\right]\log_2 e. \qquad (117)\end{aligned}$$

where η is the MMSE multiuser efficiency satisfying (67).

If the channel is ergodic in frequency, then the above conditioned capacity coincides with its unconditioned (ergodic) value.

Specializing the explicit expression of the first and second normalized moments of the matrix $\frac{1}{Q}\tilde{\boldsymbol{S}}\tilde{\boldsymbol{S}}^\dagger$ to the downlink, using $\mathrm{E}[|\mathsf{A}|^2] = \mathrm{E}[|\mathsf{H}|^2] = 1$, we have (cf. [14])

$$\begin{aligned}\lim_{N\to\infty}\frac{1}{NQ}\mathrm{Tr}\left\{\tilde{\boldsymbol{S}}\tilde{\boldsymbol{S}}^\dagger\right\} &= \beta \\ \lim_{N\to\infty}\frac{1}{NQ^2}\mathrm{Tr}\left\{\left(\tilde{\boldsymbol{S}}\tilde{\boldsymbol{S}}^\dagger\right)^2\right\} &= \beta\mathrm{E}[(|\mathsf{A}|^2)^2] + \beta^2\mathrm{E}[(|\mathsf{H}|^2)^2].\end{aligned} \tag{118}$$

Proceeding as done for the uplink

$$\frac{E_b}{N_0}_{\min} = \log_e 2 \tag{119}$$

and

$$S_0^{\mathsf{opt}} = \frac{2\beta}{\beta\kappa(|\mathsf{H}|) + \kappa(|\mathsf{A}|)} \tag{120}$$

while

$$S_\infty^{\mathsf{opt}} = \min\{\beta|\mathsf{A}|^+, |\mathsf{H}|^+\} \tag{121}$$

from which the optimum capacity is seen to grow without bound as $\frac{E_b}{N_0} \to \infty$. Specializing (107) and (108) to the dowlink we find

$$\bar{S}_0^{\mathsf{opt}} = \frac{2\beta}{\beta\mathbb{E}[\kappa(|\mathsf{H}|)] + \kappa(|\mathsf{A}|)} \tag{122}$$

and

$$\bar{S}_{\infty}^{\mathsf{opt}} = \min\{\beta \mathsf{A}|^{+}, \mathbb{E}[|\mathsf{H}|^{+}]\}. \tag{123}$$

Thus, for channels ergodic in time the high-SNR slope shows no dependence on the subcarrier fading if $\mathbb{E}[|\mathsf{H}|^{+}] = 1$.[10] Moreover, as in the uplink, frequency-selective fading can be seen to reduce the optimum capacity with respect to that of an unfaded channel.

Next, we analyze the behavior as the number of users per subcarrier grows without bound.

Corollary 5.3: Conditioned on the fading coefficients, the optimum capacity converges as $\beta \to \infty$ to the solution of

$$\mathsf{C}_{\infty}^{\mathsf{opt}} = \mathrm{E}\left[\log_2\left(1 + \mathsf{C}_{\infty}^{\mathsf{opt}} \frac{E_b}{N_0} |\mathsf{H}|^2\right)\right]. \tag{124}$$

From (124), applying Jensen's inequality to the concave function $\log_2(1+x)$

$$\mathsf{C}_{\infty}^{\mathsf{opt}} \leq \log_2\left(1 + \mathsf{C}_{\infty}^{\mathsf{opt}} \frac{E_b}{N_0}\right) \tag{125}$$

which can be rewritten as

$$\frac{2^{\mathsf{C}_{\infty}^{\mathsf{opt}}} - 1}{\mathsf{C}_{\infty}^{\mathsf{opt}}} \leq \frac{E_b}{N_0}. \tag{126}$$

For temporally ergodic channels, in terms of $\frac{E_b^t}{N_0}$

$$\bar{\mathsf{C}}_{\infty}^{\mathsf{opt}} = \mathbb{E}\left[\mathrm{E}\left[\log_2\left(1 + \bar{\mathsf{C}}_{\infty}^{\mathsf{opt}} \frac{E_b^t}{N_0} Q_y Q_x |\mathsf{H}|^2\right)\right]\right] \tag{127}$$

from which, applying Jensen's inequality

$$\bar{\mathsf{C}}_{\infty}^{\mathsf{opt}} \leq \mathbb{E}\left[\log_2\left(1 + \bar{\mathsf{C}}_{\infty}^{\mathsf{opt}} \frac{E_b^t}{N_0} Q_y Q_x\right)\right]. \tag{128}$$

The inequality (128) becomes a strict equality if the fading is either absent or frequency flat and, thus, the corresponding capacities coincide with the right-hand side of (128) as the load factor becomes large. Consequently, in this high-load regime, the fact that the fading is selective in frequency can only have a detrimental effect.

Figs. 4 and 5 show the optimum capacity as function of $\frac{E_b}{N_0}$ for both unfaded and frequency-selective faded channels with $\beta = 0.6$ and $\beta = 2.5$. The asymptotic empirical distribution of the eigenvalues of $\boldsymbol{A}\boldsymbol{A}^{\dagger}$ and of the subcarrier fading coefficients are the same as those used in Figs. 1 and 2. Fig. 6 depicts the optimum capacity for the same channel as a function of β for $\frac{E_b}{N_0} = 10$ dB.

The figures can also be explained more generally using our results for the uplink. From the derivative of the optimum capacity given in (198) in the Appendix, Part E and the fixed-point equation (22), it is readily seen invoking Jensen's inequality that nonuniformities in the variances of the entries of $\tilde{\boldsymbol{S}}$ reduce the derivative and therefore the optimum capacity itself. Thus, the fact that frequency-selective fading reduces the capacity with respect to no fading holds for any β and snr. In turn, the detrimental effect of frequency selectivity over flat fading holds for $\beta \to \infty$.

As in the linear MMSE case, also for the optimum receiver the factorization of the channel profile function that leads to the simplified form of the downlink results applies—asymptotically—to the uplink in the case of statistically symmetric users and ergodicity in frequency, leading again to a reformulation that coincides with the unfaded channel spectral efficiency. To obtain that solution it is enough to use the results in this section with $|\mathsf{H}| = 1$ while $|\mathsf{A}|^2$ is a random variable whose distribution is the asymptotic spectrum of $\frac{1}{Q_y}\boldsymbol{A}\boldsymbol{A}^{\dagger}$.

VI. Decorrelator

Next, we consider a bank of decorrelators followed by single-user decoders. Decorrelators completely null out MAI by projecting the received vector $\boldsymbol{r}$ onto the subspace orthogonal to the interfering users. A bank of decorrelators outputs [33]

$$\boldsymbol{r}' = \boldsymbol{b} + \boldsymbol{n}' \tag{129}$$

where $\boldsymbol{n}'$ is a colored Gaussian noise vector with zero mean and covariance matrix given by $\sigma^2(\tilde{\boldsymbol{S}}^{\dagger}\tilde{\boldsymbol{S}})^{-1}$. From the definition of multiuser efficiency, the instantaneous SINR of user k at the output of the decorrelator is

$$\mathsf{SINR}_k = \frac{\|\tilde{\boldsymbol{s}}_k\|^2}{\sigma^2} \eta_k^{\mathsf{dec}} \tag{130}$$

where η_k^{dec} is the instantaneous decorrelator multiuser efficiency of user k, which equals the MMSE multiuser efficiency as the background noise vanishes, i.e.,

$$\eta_k^{\mathsf{dec}} = \lim_{\sigma^2 \to 0} \eta_k^{\mathsf{mmse}}. \tag{131}$$

Because of the absence of MAI at the decorrelator output, the asymptotic spectral efficiency is

$$\mathsf{C}^{\mathsf{dec}} = \lim_{K \to \infty} \frac{1}{N} \sum_{k=1}^{K} \log_2\left(1 + \frac{\|\tilde{\boldsymbol{s}}_k\|^2}{\sigma^2} \eta_k^{\mathsf{dec}}\right). \tag{132}$$

A. Uplink

From (131), using Property 4.3, it follows that for $K, N \to \infty$ with $\frac{K}{N} \to \beta$, denoted by y' the normalized index of the kth user (i.e., $k = \lfloor y' K \rfloor$), we have the following.

Theorem 6.1: If $\beta' < 1$, with β' as defined in (38), then η_k^{dec} converges to the solution of

$$\eta(y') = \mathrm{E}\left[\frac{\varrho(\mathsf{X}, y')}{1 + \beta \mathrm{E}\left[\frac{\varrho(\mathsf{X},\mathsf{Y})}{\eta(\mathsf{Y})}|\mathsf{X}\right]}\right] \tag{133}$$

with $\varrho(\cdot,\cdot) = \frac{\rho(\cdot,\cdot)}{\mathrm{E}[\rho_k(\mathsf{X})]}$ and with X and Y independent random variables uniform on $[0,1]$ and $[0,\beta]$, respectively.

Since, as shown in Section IV-A, for channels ergodic in frequency the MMSE multiuser efficiency is reduced in the presence of frequency selectivity with respect to the case of no fading, the decorrelator multiuser efficiency is also reduced. Theorem 6.1, in conjunction with (132), yields the following.

[10] Recall that $\mathbb{E}[|\mathsf{H}|^{+}] = 1$ indicates that for almost every fading realization the fraction of subcarriers that are inactive is vanishingly small.

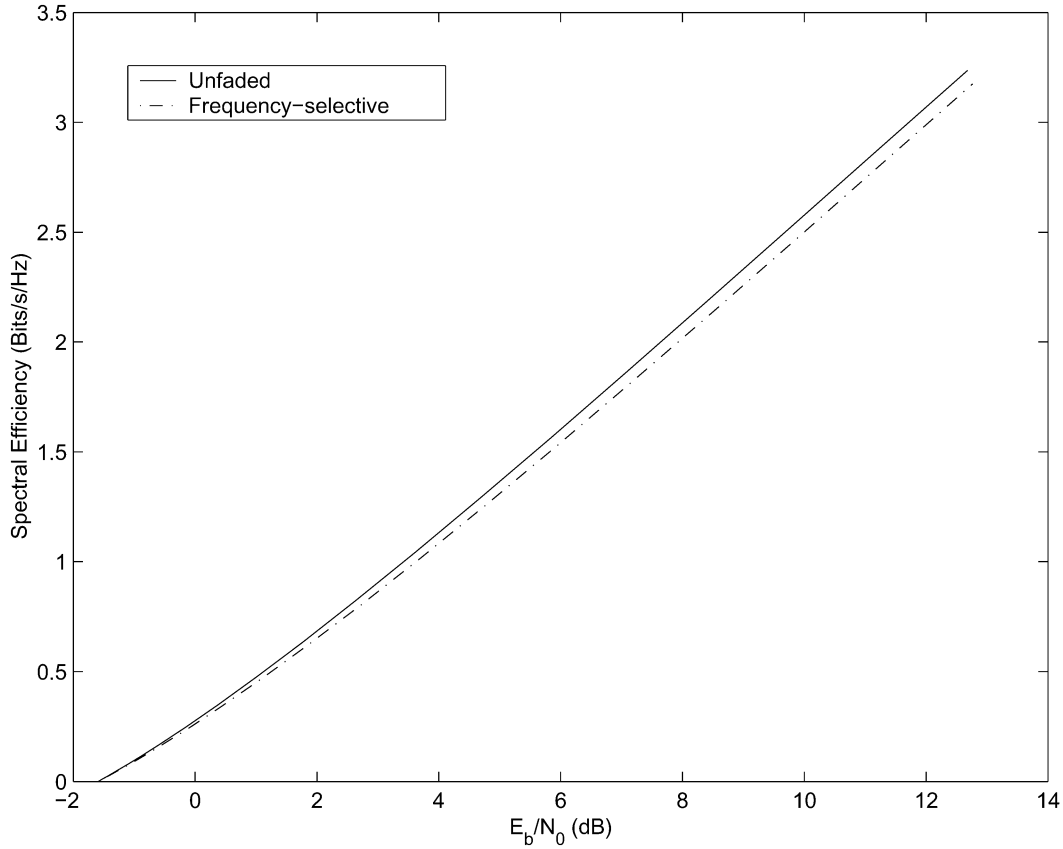

Fig. 4. Optimum capacity for $\beta = 0.6$.

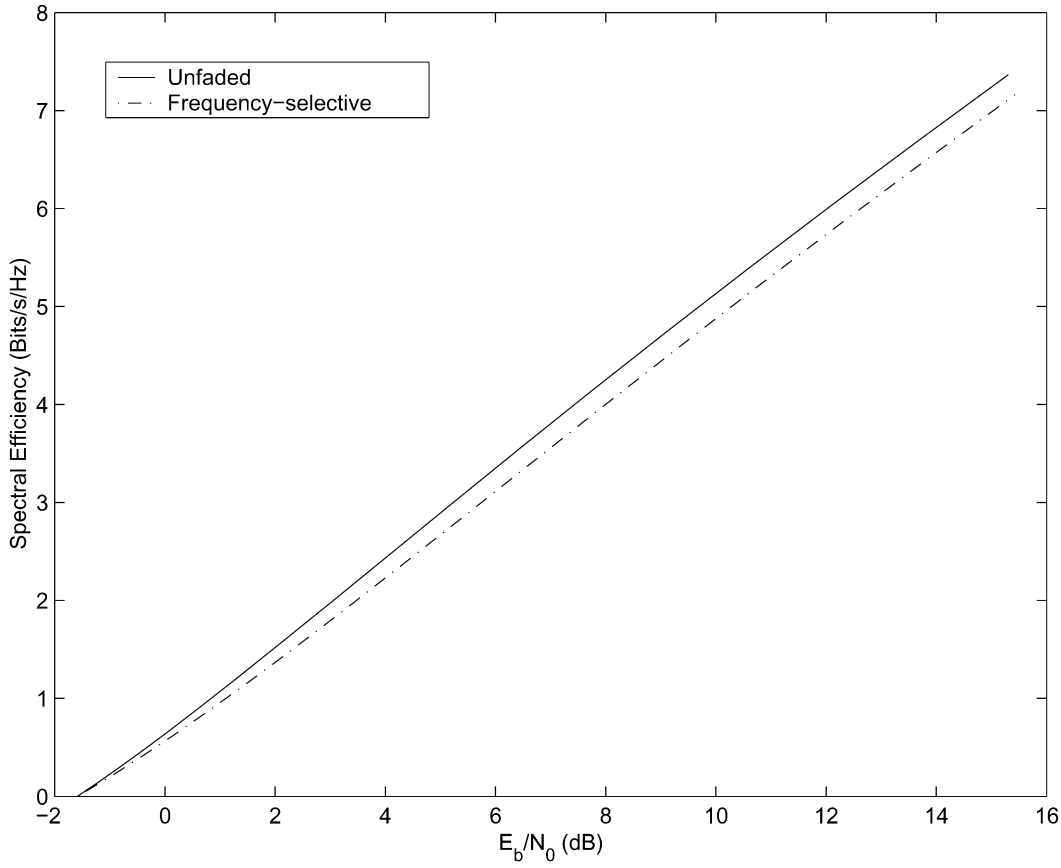

Fig. 5. Optimum capacity for $\beta = 2.5$.

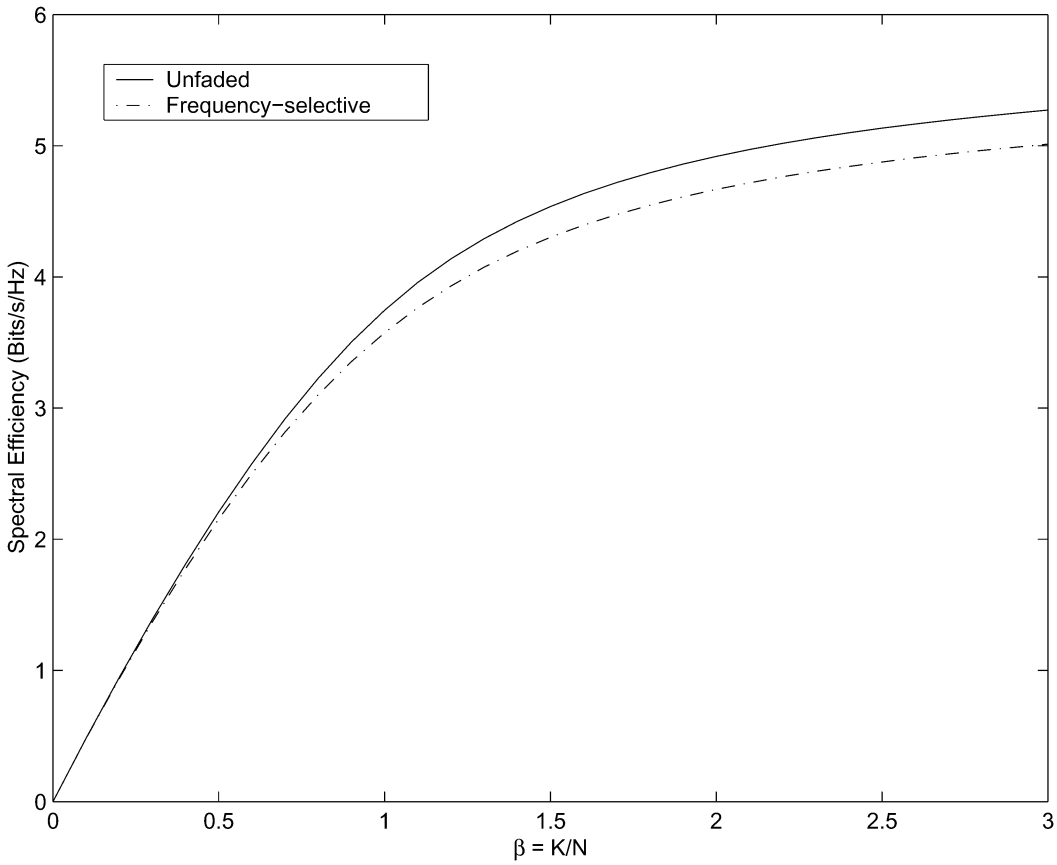

Fig. 6. Optimum capacity for $\frac{E_b}{N_0} = 10$ dB.

Theorem 6.2: Conditioned on the fading coefficients, for $\beta' < 1$ the spectral efficiency of the decorrelator converges almost surely to

$$\mathsf{C}^{\mathsf{dec}} = \int_0^{\beta} \log_2 \left(1 + \mathsf{snr}\mu^{\mathsf{dec}}(y')\right) dy' \tag{134}$$

with $\mu^{\mathsf{dec}}(\cdot)$ satisfying

$$\mu^{\mathsf{dec}}(y') = \mathrm{E}\left[\frac{\rho(\mathsf{X}, y')}{1 + \beta \mathrm{E}\left[\frac{\rho(\mathsf{X},\mathsf{Y})}{\mu^{\mathsf{dec}}(\mathsf{Y})}|\mathsf{X}\right]}\right]. \tag{135}$$

The minimum received $\frac{E_b}{N_0}$ needed for reliable communication can also be readily calculated as

$$\frac{E_b}{N_0}_{\min} = \lim_{\mathsf{snr}\to 0} \frac{\beta \mathsf{snr}}{\mathsf{C}^{\mathsf{dec}}(\mathsf{snr})} \tag{136}$$

$$= \frac{\beta}{\dot{\mathsf{C}}^{\mathsf{dec}}(0)} \tag{137}$$

$$= \frac{\log_e 2}{\mathrm{E}[\mu^{\mathsf{dec}}(\mathsf{Y})]} \tag{138}$$

where $\mu^{\mathsf{dec}}(\cdot)$ satisfies (135). From (138), the reduction in decorrelator multiuser efficiency due to frequency-selective fading translates into a stricter $\frac{E_b}{N_0}_{\min}$ requirement with respect to an unfaded channel if the fading is ergodic in frequency.

Using Property 4.4, we obtain the low- and high-SNR slope of the decorrelator spectral efficiency.

Proposition 4.1: For $\beta' < 1$, the slopes, conditioned on the fading coefficients, are given by

$$S_0^{\mathsf{dec}} = 2\beta \frac{\mathrm{E}^2[\mu^{\mathsf{dec}}(\mathsf{Y})]}{\mathrm{E}[(\mu^{\mathsf{dec}}(\mathsf{Y}))^2]} \tag{139}$$

while

$$S_\infty^{\mathsf{dec}} = \beta \Pr\{\mathcal{Z}_Y(\mathsf{Y}) \neq 0\}. \tag{140}$$

The slope counterparts for channels nonergodic in frequency but ergodic in time can be obtained following the same steps but using $\bar{\mathsf{C}}^{\mathsf{dec}}$ rather than $\mathsf{C}^{\mathsf{dec}}$ and for $\beta' < 1$ are given by

$$\bar{S}_0^{\mathsf{dec}} = 2\beta \frac{\mathbb{E}[\mathrm{E}^2[\mu^{\mathsf{dec}}(\mathsf{Y})]]}{\mathbb{E}[\mathrm{E}[(\mu^{\mathsf{dec}}(\mathsf{Y}))^2]]}$$
$$\bar{S}_\infty^{\mathsf{dec}} = \beta \mathbb{E}[\Pr\{\mathcal{Z}_Y(\mathsf{Y}) \neq 0\}]. \tag{141}$$

B. Downlink

As in previous sections, the results in Section VI-A can be specialized to the downlink.

Corollary 4.1: Conditioned on the fading coefficients, for $\beta' < 1$ the decorrelator multiuser efficiency η_0 in the downlink satisfies

$$\mathrm{E}\left[\frac{1}{1 + \frac{\beta|\mathsf{A}|^+|\mathsf{H}|^2}{\eta_0}}\right] - \frac{1 - |\mathsf{H}|^+}{|\mathsf{H}|^+} = 1 - \beta' \tag{142}$$

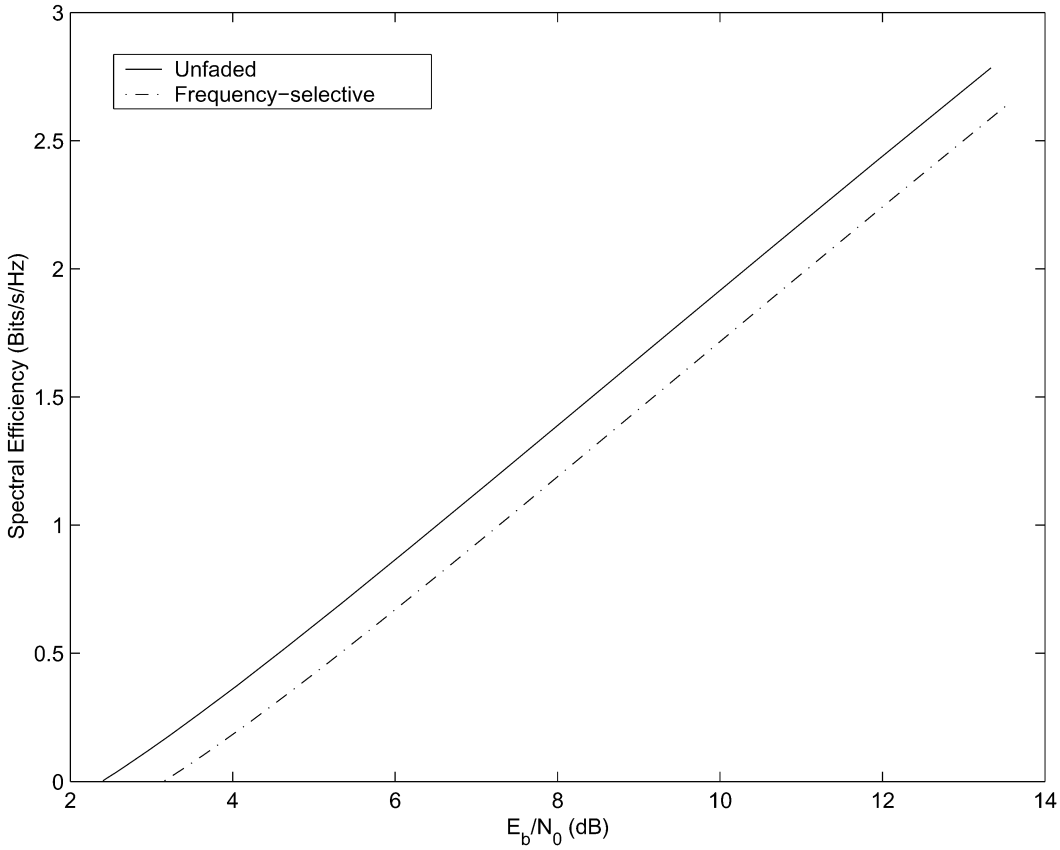

Fig. 7. Decorrelator spectral efficiency for $\beta = 0.6$.

whereas the corresponding spectral efficiency admits the expression

$$\mathsf{C}^{\mathsf{dec}} = \beta \mathrm{E}\left[\log_2\left(1 + \mathsf{snr}\eta_0|\mathsf{A}|^2\right)\right]. \tag{143}$$

In turn, the low- and high-SNR measures specialize to

$$\frac{E_b}{N_0}_{\min} = \frac{\log_e 2}{\eta_0} \tag{144}$$

$$S_0^{\mathsf{dec}} = \frac{2\beta}{\kappa(|\mathsf{A}|)} \tag{145}$$

$$S_\infty^{\mathsf{dec}} = \beta P^+. \tag{146}$$

Notice that, for $\beta' < 1$, the low- and high-SNR slopes are not affected by the fading. Their expressions coincide with those for an unfaded channel. The impact of fading at low SNR is only reflected on the minimum energy per bit, which does depend on the fading.

Figs. 7 and 8 illustrate the decorrelator spectral efficiency as a function of $\frac{E_b}{N_0}$ and β, respectively.

VII. Single-User Matched Filter

In this final section, we consider a bank of single-user matched filters followed by single-user decoders. The matched filter of user k correlates the received vector $\boldsymbol{r}$ with user k's received spreading sequence $\tilde{\boldsymbol{s}}_k$ and outputs

$$\tilde{\boldsymbol{s}}_k^\dagger \boldsymbol{r} = b_k \tilde{\boldsymbol{s}}_k^\dagger \tilde{\boldsymbol{s}}_k + \sum_{i \neq k} b_i \tilde{\boldsymbol{s}}_k^\dagger \tilde{\boldsymbol{s}}_i + \tilde{\boldsymbol{s}}_k^\dagger \boldsymbol{n}. \tag{147}$$

Recalling $\tilde{\boldsymbol{S}}_k = (\tilde{\boldsymbol{s}}_1, \ldots, \tilde{\boldsymbol{s}}_{k-1}, \tilde{\boldsymbol{s}}_{k+1}, \ldots, \tilde{\boldsymbol{s}}_K)$, the instantaneous matched-filter output SINR is

$$\mathsf{SINR}_k = \frac{\left|\tilde{\boldsymbol{s}}_k^\dagger \tilde{\boldsymbol{s}}_k\right|^2}{\tilde{\boldsymbol{s}}_k^\dagger \left(\tilde{\boldsymbol{S}}_k \tilde{\boldsymbol{S}}_k^\dagger\right) \tilde{\boldsymbol{s}}_k + \sigma^2 \tilde{\boldsymbol{s}}_k^\dagger \tilde{\boldsymbol{s}}_k}. \tag{148}$$

A. Uplink

It is shown in [20], [36], [37], using central limit arguments, that the interference distribution at the output of the matched filter is well approximated by a Gaussian function. Consequently, the spectral efficiency of the single-user matched filter can be expressed as

$$\mathsf{C}^{\mathsf{sumf}} = \lim_{K\to\infty} \beta \frac{1}{K} \sum_{k=1}^{K} \log_2\left(1 + \mathsf{SINR}_k\right). \tag{149}$$

Denote by y' the normalized index of the kth user. Almost surely [14]

$$\|\boldsymbol{s}_k\|^2 \to Q \int_0^1 \rho(x, y')dx$$

$$\tilde{\boldsymbol{s}}_k^\dagger \left(\tilde{\boldsymbol{S}}_k \tilde{\boldsymbol{S}}_k^\dagger\right) \tilde{\boldsymbol{s}}_k \to Q \int_0^1 \int_0^\beta \rho(x, y)\rho(x, y')dydx$$

from which, using (148), the following theorem ensues.

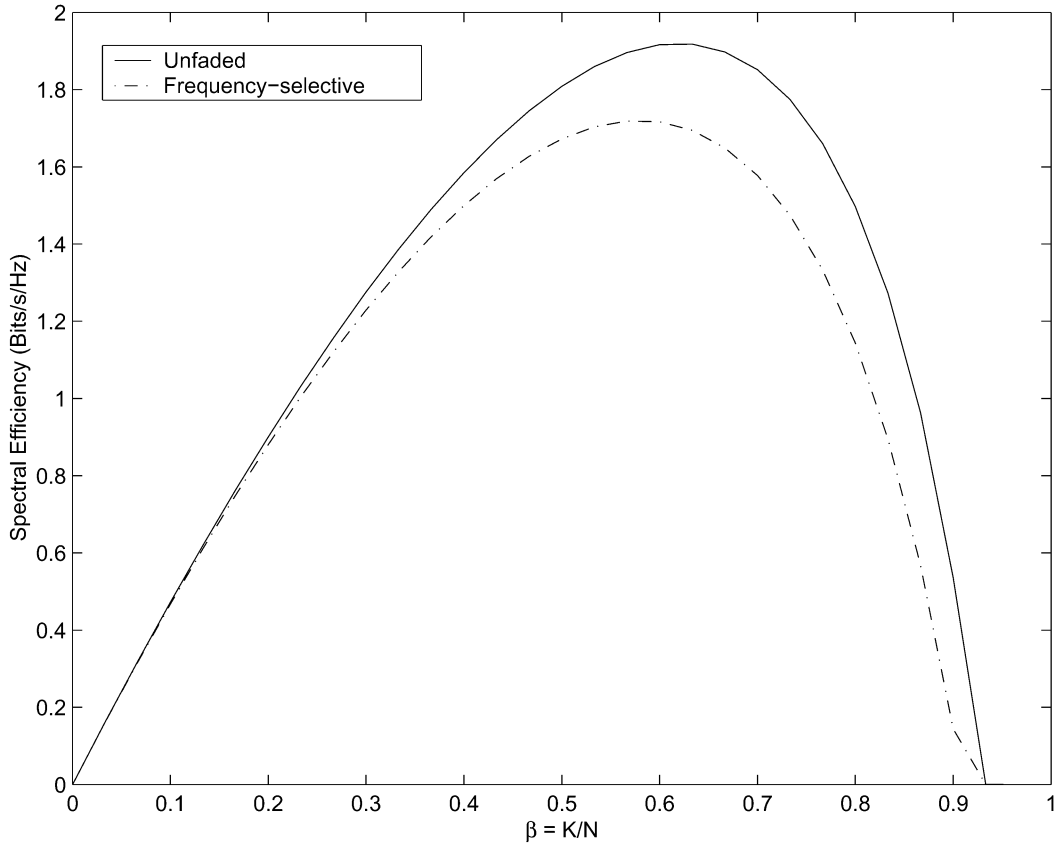

Fig. 8. Decorrelator spectral efficiency for $\frac{E_b}{N_0} = 10$ dB.

Theorem 7.1: Conditioned on the fading coefficients, the matched-filter output SINR converges almost surely as $K, N \to \infty$ with $\frac{K}{N} \to \beta$ to

$$\mathsf{SINR}_k \xrightarrow{a.s} \frac{\left(\int_0^1 \rho(x,y')dx\right)^2}{\int_0^1 dx \int_0^\beta \rho(x,y)\rho(x,y')dy + \frac{1}{\mathsf{snr}} \int_0^1 \rho(x,y')dx} \tag{150}$$

while, conditioned on the fading coefficients, the spectral efficiency of the matched filter converges almost surely to (151) at the bottom of the page.

From the preceding theorem, the following proposition is easily obtained.

Proposition 7.1: Conditioned on the fading coefficients, $\frac{E_b}{N_0}_{\min} = \log_e 2$ and

$$S_0^{\mathsf{sumf}} = \frac{2\beta}{\int_0^\beta \left(\int_0^1 \rho(x,y)dx\right)^2 dy + 2\int_0^1 \left(\int_0^\beta \rho(x,y)dy\right)^2 dx}. \tag{152}$$

Moreover, letting $\frac{E_b}{N_0} \to \infty$ we obtain

$$\mathsf{C}^{\mathsf{sumf}} = \int_0^\beta \log_2 \left(1 + \frac{\left(\int_0^1 \rho(x,y')dx\right)^2}{\int_0^1 \int_0^\beta \rho(x,y)\rho(x,y')dydx}\right) dy' \tag{153}$$

from which $S_\infty^{\mathsf{sumf}} = 0$.

Note that (152) coincides with the slope obtained for the MMSE receiver in Proposition 4.1. Furthermore, (153) confirms the well-known fact that the single-user matched filter is interference limited: its spectral efficiency is bounded even in the absence of background noise.

B. Downlink

Specializing Theorem 7.1 to the downlink, the matched-filter output SINR converges almost surely, conditioned on the fading coefficients, to

$$\frac{|A_k|^2}{Q_y} \frac{1}{\beta\kappa(|\mathsf{H}|) + \frac{1}{\mathsf{snr}}} \tag{154}$$

$$\mathsf{C}^{\mathsf{sumf}} = \int_0^\beta \log_2 \left(1 + \frac{\left(\int_0^1 \rho(x,y')dx\right)^2}{\int_0^1 \int_0^\beta \rho(x,y)\rho(x,y')dydx + \frac{1}{\mathsf{snr}} \int_0^1 \rho(x,y')dx}\right) dy'. \tag{151}$$

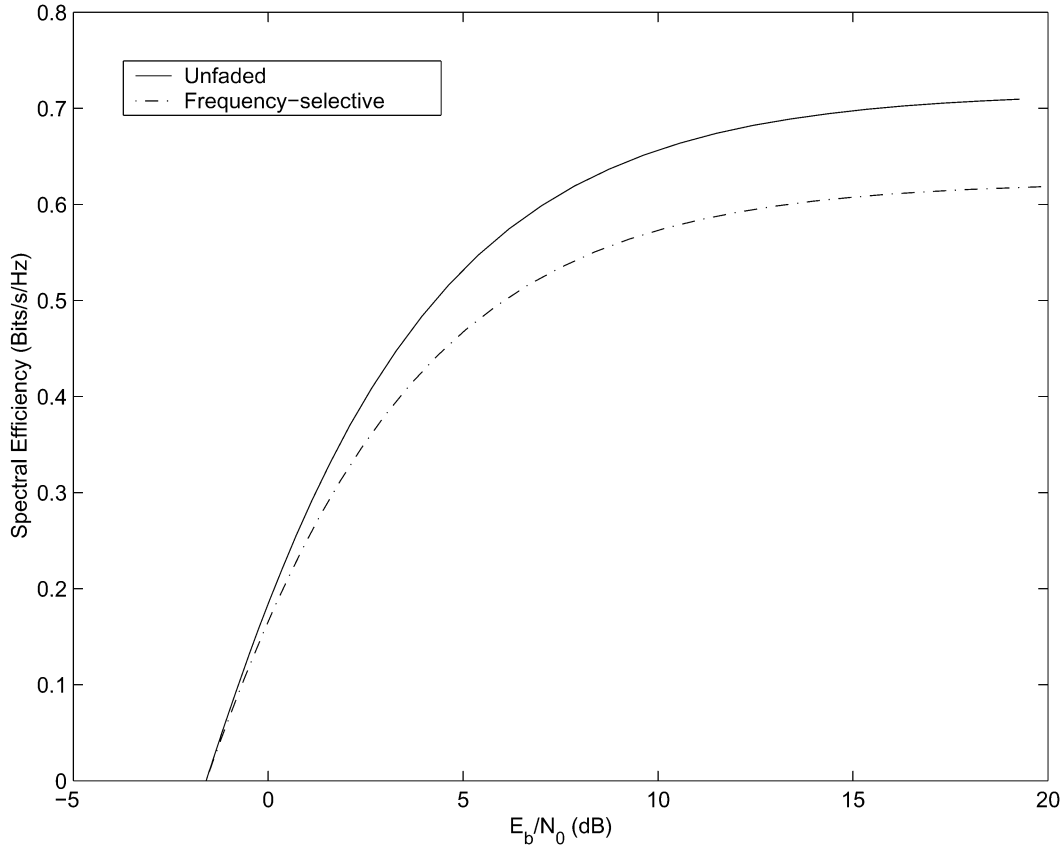

Fig. 9. Matched filter spectral efficiency for $\beta = 0.6$.

where we have used $\mathrm{E}[|\mathsf{A}|^2] = \mathrm{E}[|\mathsf{H}|^2] = 1$. For the case of unitarily invariant signature matrices, the matched-filter output SINR can be found in [11].

Analogously, the asymptotic downlink matched-filter spectral efficiency is

$$\mathsf{C}^{\mathsf{sumf}} = \beta \mathrm{E}\left[\log_2\left(1 + \frac{\mathsf{snr}|\mathsf{A}|^2}{1 + \mathsf{snr}\beta\kappa(|\mathsf{H}|)}\right)\right]. \tag{155}$$

The kurtosis in (155) is seen to reduce the matched filter spectral efficiency with respect to the one for $\kappa(|\mathsf{H}|) = 1$. Specializing Proposition 7.1 to the downlink

$$S_0^{\mathsf{sumf}} = \frac{2\beta}{2\beta\kappa(|\mathsf{H}|) + \kappa(|\mathsf{A}|)} \tag{156}$$

while $S_\infty^{\mathsf{sumf}} = 0$.

The spectral efficiency in (155) is not only monotonically increasing in snr but also in β. For temporally ergodic channels, its limiting value as β grows without bound, $\lim_{\beta\to\infty} \bar{\mathsf{C}}^{\mathsf{sumf}} = \bar{\mathsf{C}}_\infty^{\mathsf{sumf}}$, satisfies

$$1 = \mathbb{E}\left[\frac{Q_y Q_x}{1 + \bar{\mathsf{C}}_\infty^{\mathsf{sumf}} \frac{E_b}{N_0}\kappa(|\mathsf{H}|)}\right] \tag{157}$$

which in the case of channels ergodic in frequency, where $\mathbb{E}[\cdot]$ with respect to the subcarrier fading distribution is immaterial, can be rewritten as

$$\mathsf{C}_\infty^{\mathsf{sumf}} = \frac{1}{\kappa(|\mathsf{H}|)}\left(\log_2 e - \frac{N_0}{E_b}\right). \tag{158}$$

From (157), fading has a direct impact on the high-load behavior of the spectral efficiency. For frequency ergodic channels with Rayleigh distribution, where the kurtosis is 2, the matched filter spectral efficiency in the high-load regime is only half that of an unfaded system (cf. (158)).

Figs. 9–11 show the matched filter spectral efficiency as a function of $\frac{E_b}{N_0}$ and β. Comparing these figures with those for the other receivers, we conclude that the matched filter is much more sensitive to the subcarrier fading.

VIII. Conclusions

This paper has analyzed the spectral efficiency of several receivers for MC-CDMA channels subject to frequency-selective fading. For both uplink and downlink, we have analyzed the spectral efficiency conditioned/unconditioned on the fading realization for nonergodic/ergodic channels, respectively. The conditioned spectral efficiency, in particular, has been shown to converge asymptotically in the number of users and subcarriers to an expression that depends on the empirical instantaneous fading profile across the subcarriers. This is a versatile result that transcends wireless channels and that may be of interest to other potential applications of MC-CDMA such as wireline communication. Although, throughout the paper, the fading experienced by a given user has been considered identically distributed at each subcarrier, most of the results extend immediately to instances where the fading is nonidentically

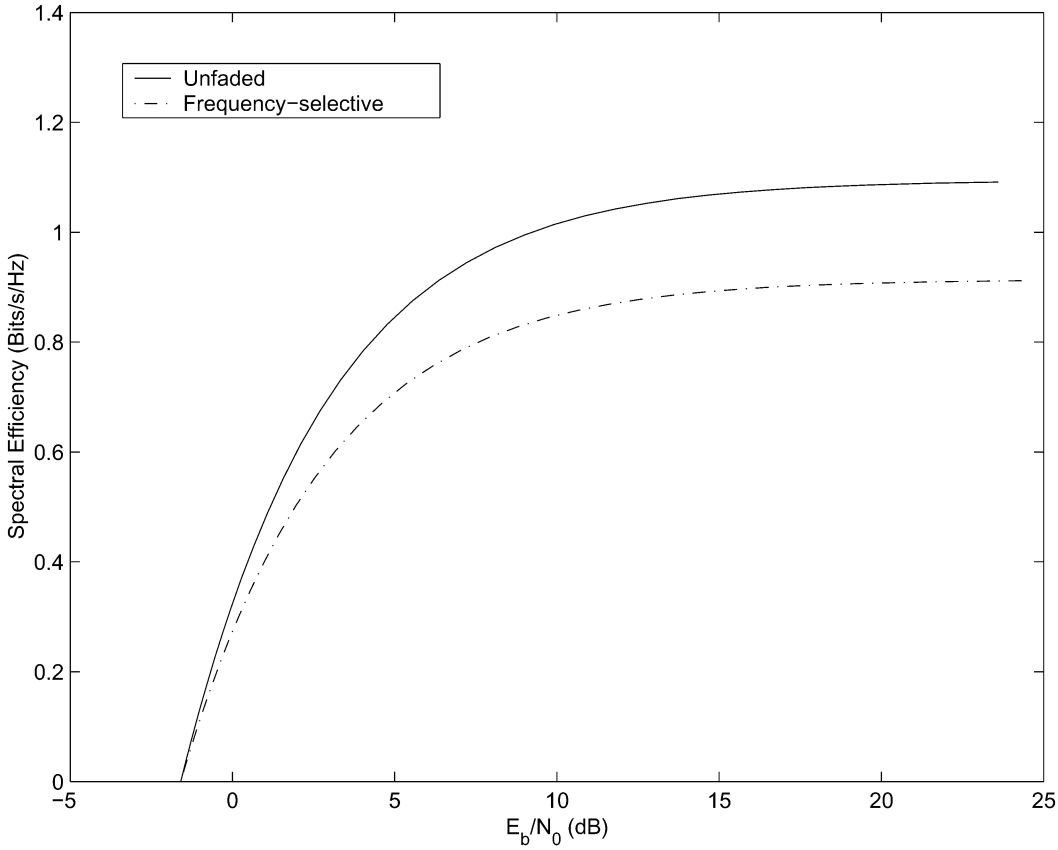

Fig. 10. Matched filter spectral efficiency for $\beta = 2.5$.

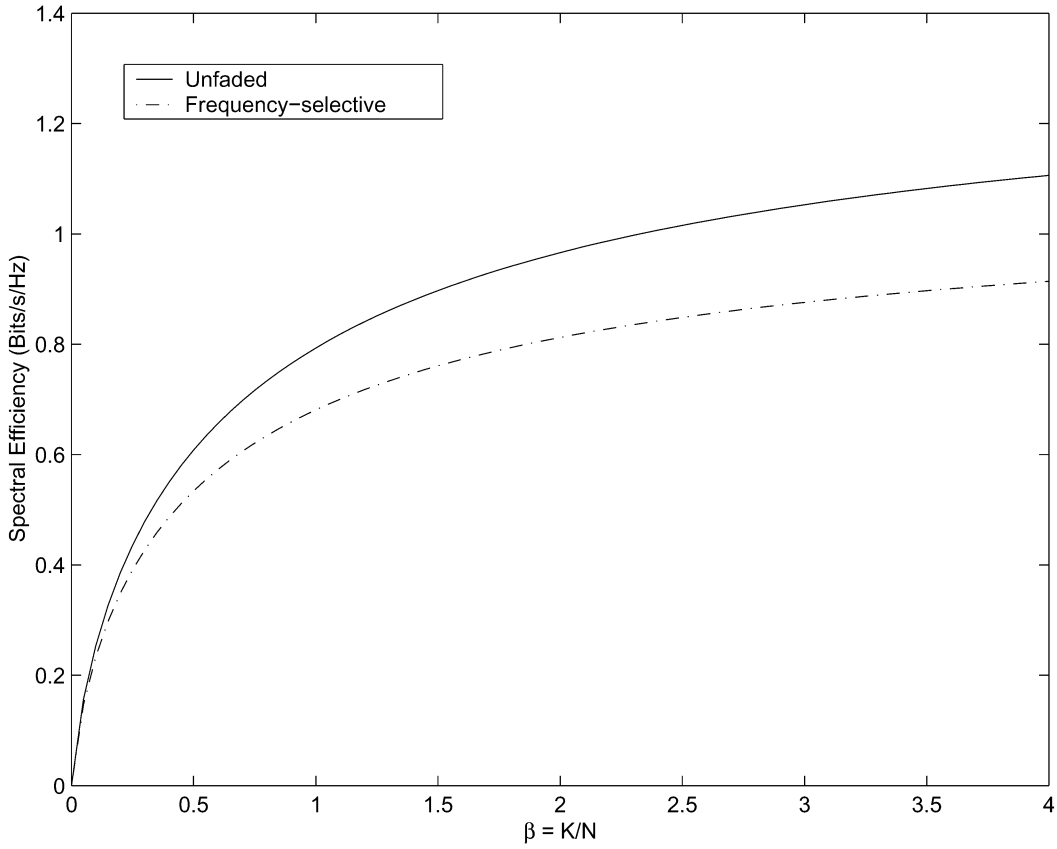

Fig. 11. Matched filter spectral efficiency for $\frac{E_b}{N_0} = 10$ dB.

distributed across the subcarriers. This would enable accommodating disparities in the noise variance that may arise because of cochannel interference.

One of our main findings is the expression characterizing the extra efficiency attained when going from optimum linear to optimum nonlinear processing as a function of the uncoded linear MMSE performance measure.

The effect of frequency-selective fading on the spectral efficiency of several multiuser receivers has also been studied. Our results show that frequency-selective fading, like frequency-flat fading, results in a loss with respect to the corresponding unfaded channel. Since the minimum received energy per bit required to communicate reliably is unaffected, the loss is manifested at low SNR as a reduction in the slope of the spectral efficiency versus energy per bit function in the vicinity of such minimum energy. At high SNR, in contrast, the slope of the spectral efficiency function is not altered by frequency-selective fading except in the case that a nonvanishing fraction of the subcarriers are completely inactive for every user, i.e., the channel response at those frequencies is exactly zero for every user. Therefore, the impact of frequency-selective fading at high SNR is in general captured, not by the slope, but by the zero-order term in the corresponding expansion. This term, first analyzed in [23] for flat-faded channels, can be characterized for frequency-selective MC-CDMA uplink and downlink using [29, Theorems 2.45 and 2.54] (see also [27] for a similar characterization in the context of multiple-antenna communications). Also noteworthy is that the loss associated with frequency-selective fading is more pronounced for the single-user matched filter than for the optimum receiver, MMSE receiver and decorrelator. Therefore, exploiting the MAI structure in the receiver design is beneficial, not only to increase the spectral efficiency, but to desensitize against the impact of frequency-selective fading.

Some statements have also been made on the relative impact of frequency-selective fading with respect to that of frequency-flat fading. Although, in general, frequency selectivity is regarded as favorable, we have shown that it need not always be the case in large systems. Specifically, if the channel is ergodic in either frequency or time, then once the number of users becomes much larger than the number of subcarriers, selectivity in frequency becomes detrimental. Indeed, its negative effect (mitigation of the fading exhibited by interfering users) outweighs its positive effect (mitigation of fading experienced by the user of interest).

The results presented in this paper apply directly to frequency-selective DS-CDMA systems with negligible ISI in the case of randomly spread chips with Gaussian distribution. For non-Gaussian distributions, the results still apply using [29, Theorem 2.43].

Technically, the asymptotic analysis of the MC-CDMA uplink has required sharper tools than the ones used for flat-faded MC-CDMA. While, in the latter, the Marcenko–Pastur framework [16] was shown in [23] to be sufficient, here the more general framework by Girko [8] proves to be instrumental in the key technical results [29]. Girko's theorem (already applied in [4] to multiple-antenna channels with spatially correlated fading and in [12] to CDMA networks with multiuser receivers and spatial diversity) can be seen as a generalization of the Silverstein–Bai theorem [1]. The former gives the Stieltjes transform of a random matrix whose entries are zero-mean independent and nonidentically distributed with a variance matrix having a totally general structure while, in the latter, the variance matrix corresponds to the outer product of two suitable vectors. Whereas the more general Girko result has to be invoked in the MC-CDMA uplink, for the corresponding downlink—derived as a special case thereof—the more restrictive Silverstein–Bai theorem suffices.

APPENDIX

A. Mathematical Background

Theorem 8.1: [8], [10], [24] Define an $N \times K$ matrix $\boldsymbol{H}$ whose entries are zero-mean independent complex random variables. Let their second moments be

$$\mathrm{E}[|\mathsf{H}_{i,j}|^2] = \frac{\mathsf{P}_{i,j}}{N} \tag{159}$$

with $\boldsymbol{P}$ an $N \times K$ deterministic matrix whose entries are uniformly bounded. As $K, N \to \infty$ with $K/N \to \beta$, the empirical eigenvalue distribution of $\boldsymbol{H}\boldsymbol{H}^\dagger$ converges almost surely to a limiting distribution whose Stieltjes transform is

$$\mathcal{S}_{\boldsymbol{H}}(z) = \lim_{N\to\infty} \frac{1}{N} \mathrm{Tr} \left\{ \left(\boldsymbol{I} + z\boldsymbol{H}\boldsymbol{H}^\dagger \right)^{-1} \right\} = \int_0^1 v(x,z)dx \tag{160}$$

with $v(\cdot,\cdot)$ solution to the fixed point equation

$$v(x,z) = \frac{1}{1 + z\int_0^\beta \frac{\rho_{\boldsymbol{P}}(x,y)}{1+z\int_0^1 v(w,z)\rho_{\boldsymbol{P}}(w,y)dw} dy} \tag{161}$$

where $\rho_{\boldsymbol{P}}(\cdot,\cdot)$ is the channel profile function of $\boldsymbol{P}^{\frac{1}{2}}$ as defined in Section II.

The solution to the above equation exists and is unique in the class of functions $v(x,z)$ that are analytical in z and continuous on $0 \le x \le 1$.

The next theorem is direct consequence of Theorem 2.1.

Theorem 8.2: [27], [29] Let $\boldsymbol{V} = \boldsymbol{B} \circ \boldsymbol{D}$ be an $N \times K$ matrix with $\circ$ denoting Hadamard (element-wise) product and with $\boldsymbol{B}$ and $\boldsymbol{D}$ independent $N \times K$ random matrices. The entries of $\boldsymbol{B}$ are zero-mean i.i.d. complex, arbitrarily distributed, and with variance $1/N$, while $\boldsymbol{D}$ is as in Definition 2.2 with $F_x(\cdot)$ and $F_y(\cdot)$ having all their moments bounded. Further, define

$$\mathcal{F}^{(N)}(y,\gamma) = \boldsymbol{v}_j^\dagger \left(\boldsymbol{I} + \gamma \sum_{\ell \ne j} \boldsymbol{v}_\ell \boldsymbol{v}_\ell^\dagger \right)^{-1} \boldsymbol{v}_j, \quad \frac{j-1}{N} \le y < \frac{j}{N}$$

with $\boldsymbol{v}_j$ denoting the jth column of $\boldsymbol{V}$. Conditioned on $\boldsymbol{D}$, as $K, N \to \infty$, $\mathcal{F}^{(N)}(y,\gamma)$ converges almost surely to $\mathcal{F}(y,\gamma)$, with $\mathcal{F}(\cdot,\gamma)$ solution to the fixed-point equation

$$\mathcal{F}(y,\gamma) = \int_0^1 \frac{\rho_{\boldsymbol{D}}(x,y)}{1 + \gamma\int_0^\beta \frac{\rho_{\boldsymbol{D}}(x,y')}{1+\gamma\mathcal{F}(y',\gamma)} dy'} dx \tag{162}$$

where $\rho_{\boldsymbol{D}}(\cdot,\cdot)$ is the channel profile function of $\boldsymbol{D}$.

Theorem 8.2 is proved in [27]. For convenience, we repeat the proof here.

Proof: Note that

$$\boldsymbol{v}_j = \mathrm{diag}(D_{1,j}, \ldots, D_{N,j})\boldsymbol{b}_j$$

where $\boldsymbol{b}_j$ denotes the jth column of $\boldsymbol{B}$. For $\alpha > 0$, define

$$D_{i,j}^{\alpha} = D_{i,j} 1\{|D_{i,j}| \leq \alpha\}$$

with $1\{\cdot\}$ the indicator function and denote with $\boldsymbol{v}^{\alpha}$ the N-dimensional vector

$$\boldsymbol{v}_j^{\alpha} = \mathrm{diag}\left(D_{1,j}^{\alpha}, \ldots, D_{N,j}^{\alpha}\right)\boldsymbol{b}_j.$$

Denote with

$$F^{(N,\alpha)}(y,\gamma) = \left(\boldsymbol{v}_j^{\alpha}\right)^{\dagger}\left(\boldsymbol{I} + \gamma\sum_{\ell\neq j}\boldsymbol{v}_{\ell}\boldsymbol{v}_{\ell}^{\dagger}\right)^{-1}\boldsymbol{v}_j^{\alpha}. \quad (163)$$

From the Moment Convergence Theorem, using [25, Lemma 2.5a] and the fact that

$$\mathrm{rank}(\boldsymbol{AB}) \leq \min(\mathrm{rank}(\boldsymbol{A}), \mathrm{rank}(\boldsymbol{B}))$$

for rectangular matrices $\boldsymbol{A}$ and $\boldsymbol{B}$ such that $\boldsymbol{AB}$ is defined, for all i and γ

$$\left|F^{(N)}(y,\gamma) - F^{(N,\alpha)}(y,\gamma)\right| \leq \frac{2}{N}\mathrm{rank}\left(\mathrm{diag}(D_{1,j},\ldots,D_{N,j}) - \mathrm{diag}(D_{1,j}^{\alpha},\ldots,D_{N,j}^{\alpha})\right) \quad (164)$$

$$= \frac{2}{N}\sum_{i=1}^{N} 1\{|D_{i,j}| > \alpha\} \quad (165)$$

$$\to 2F_j([0,\alpha]^c) \quad (166)$$

with $F_j(\cdot)$ the asymptotic empirical distribution of the N-dimensional vector $[|D_{1,j}|^2, \ldots, |D_{N,j}|^2]$ and with $[0,\alpha]^c$ such that $[0,\alpha]\cup[0,\alpha]^c \equiv [0,\infty[$. If $\alpha \to \infty$, then for all i and γ

$$\left|F^{(N)}(y,\gamma) - F^{(N,\alpha)}(y,\gamma)\right| \to 0. \quad (167)$$

For convenience, in the following we use $\mathsf{P}_{i,j} = |D_{i,j}|^2$ and $\mathsf{P}_{i,j}^{\alpha} = |D_{i,j}^{\alpha}|^2$. Recalling that $\frac{j-1}{N} \leq y < \frac{j}{N}$ and using [1, Lemma 2.7]

$$\mathbb{E}\left[\left|F^{(N\alpha)}(y,\gamma) - \frac{1}{N}\sum_{i=1}^{N}\mathsf{P}_{i,j}^{\alpha}\left(\boldsymbol{I} + \gamma\sum_{q\neq j}\boldsymbol{v}_q\boldsymbol{v}_q^{\dagger}\right)^{-1}_{i,i}\right|^2\right] \leq \frac{K}{N^2} \quad (168)$$

with K a constant that does not depend on N, $\boldsymbol{P}$, or $(\boldsymbol{I} + \gamma\sum_{q\neq j}\boldsymbol{v}_q\boldsymbol{v}_q^{\dagger})$, and with $\boldsymbol{v}_q$ the qth column of $\boldsymbol{V}$. Note that

$$\frac{1}{N}\sum_{i=1}^{N}\mathsf{P}_{i,j}^{\alpha}\left(\boldsymbol{I} + \gamma\sum_{q\neq j}\boldsymbol{v}_q\boldsymbol{v}_q^{\dagger}\right)^{-1}_{i,i} = \frac{1}{N}\sum_{i=1}^{N}\frac{\mathsf{P}_{i,j}^{\alpha}}{1 - \gamma\boldsymbol{w}_i^{\dagger}\left(\bar{\boldsymbol{I}} + \bar{\boldsymbol{W}}_i\right)^{-1}\boldsymbol{w}_i + \gamma||\boldsymbol{v}^i||^2}$$

where $\boldsymbol{v}^i$ denotes the ith row of $\boldsymbol{V}$, $\boldsymbol{w}_i$ indicates the ith column of $\sum_{q\neq j}\boldsymbol{v}_q\boldsymbol{v}_q^{\dagger}$ excluding the ith entry, while $\bar{\boldsymbol{W}}_i$ indicates the $(N-1)\times(N-1)$ submatrix obtained by eliminating from $\sum_{q\neq j}\boldsymbol{v}_q\boldsymbol{v}_q^{\dagger}$ the ith column and the ith row. Further, defining

$$\mathcal{G}^{(N)}(i,\gamma) = \left(\bar{\boldsymbol{I}} + \gamma\sum_{q\neq j}\boldsymbol{v}_q\boldsymbol{v}_q^{\dagger}\right)^{-1}_{i,i}$$

and

$$\varpi^{(N)}(i,\gamma) = \frac{\gamma}{N}\sum_{k=1}^{K}\frac{\mathsf{P}_{i,k}}{1 + \frac{\gamma}{N}\sum_{\ell=1}^{N}\mathsf{P}_{\ell,k}\mathcal{G}^{(N)}(\ell,\gamma)}$$

we can write

$$\frac{1}{N}\sum_{i=1}^{N}\mathsf{P}_{i,j}^{\alpha}\mathcal{G}^{(N)}(i,\gamma) = \frac{1}{N}\sum_{i=1}^{N}\frac{\mathsf{P}_{i,j}^{\alpha}}{1 + \varpi^{(N)}(i,\gamma) + \epsilon^{(N)}(i,\gamma)} = \frac{1}{N}\sum_{i=1}^{N}\frac{\mathsf{P}_{i,j}^{\alpha}}{1 + \varpi^{(N)}(i,\gamma)} - \delta^{(N)}(i,\gamma)$$

with

$$\epsilon^{(N)}(i,\gamma) = -\gamma\boldsymbol{w}_i^{\dagger}\left(\boldsymbol{I} + \boldsymbol{W}_i\right)^{-1}\boldsymbol{w}_i + \gamma||\boldsymbol{v}^i||^2 - \varpi^{(N)}(i,\gamma)$$

and

$$\delta^{(N)}(i,\gamma) = \frac{1}{N}\sum_{i=1}^{N}\frac{\epsilon^{(N)}(i,\gamma)\mathsf{P}_{i,j}^{\alpha}}{(1 + \varpi^{(N)}(i,\gamma))(1 + \varpi^{(N)}(i,\gamma) + \epsilon^{(N)}(i,\gamma))}.$$

Since $\mathsf{P}_{i,j}^{\alpha} \leq \log N$, it follows that

$$\delta^{(N)}(i,\gamma) \leq \frac{\log N}{N}\cdot\sum_{i=1}^{N}\frac{\epsilon^{(N)}(i,\gamma)}{(1 + \varpi^{(N)}(i,\gamma))(1 + \varpi^{(N)}(i,\gamma) + \epsilon^{(N)}(i,\gamma))} \quad (169)$$

and, invoking Theorem 2.1, we have that for fixed γ, conditioned on $\boldsymbol{D}$, almost surely

$$|\delta^{(N)}(i,\gamma)| \leq o(1)$$

and consequently

$$\lim_{N\to\infty}\frac{1}{N}\sum_{i=1}^{N}\mathsf{P}_{i,j}^{\alpha}\mathcal{G}^{(N)}(i,\gamma) = \lim_{N\to\infty}\frac{1}{N}\sum_{i=1}^{N}\frac{\mathsf{P}_{i,j}^{\alpha}}{1 + \frac{\gamma}{N}\sum_{k=1}^{K}\frac{\mathsf{P}_{i,k}}{1+\frac{\gamma}{N}\sum_{\ell=1}^{N}\mathsf{P}_{\ell,k}\mathcal{G}^{(N)}(\ell,\gamma)}}. \quad (170)$$

Denoting

$$F(y,\gamma) = \lim_{N\to\infty}\frac{1}{N}\sum_{i=1}^{N}\mathsf{P}_{i,j}^{\alpha}\mathcal{G}^{(N)}(i,\gamma)$$

with $\frac{j-1}{N} \leq y < \frac{j}{N}$, we have, from (167) and (168) and using the first Borel–Cantelli lemma [2], that almost surely

$$\lim_{N\to\infty}F^{(N)}(y,\gamma) \overset{\text{a.s.}}{=} F(y,\gamma) = \int_0^1 \rho_{\boldsymbol{D}}(x,y)v(x,\gamma)dx \quad (171)$$

with $v(\cdot,\cdot)$ satisfying the fixed-point equation in (161) or, equivalently, with $\digamma(\cdot,\gamma)$ satisfying

$$\digamma(y,\gamma)=\int_0^1 \frac{\rho_{\boldsymbol{D}}(x,y)}{1+\gamma\int_0^\beta \frac{\rho_{\boldsymbol{D}}(x,y')}{1+\gamma\digamma(y',\gamma)}dy'}dx$$

from which (162) follows.

B. Proof of Theorem 4.1

From (18), as $K,N\to\infty$

$$\begin{aligned}\eta_k&=\lim_{K\to\infty}\frac{\mathsf{SINR}_k}{\frac{||\tilde{\boldsymbol{s}}_k||^2}{\sigma^2}}\\&=\lim_{K\to\infty}\frac{\tilde{\boldsymbol{s}}_k^\dagger\left(\frac{\mathsf{snr}}{Q}\tilde{\boldsymbol{S}}_k\tilde{\boldsymbol{S}}_k^\dagger+\boldsymbol{I}\right)^{-1}\tilde{\boldsymbol{s}}_k}{||\tilde{\boldsymbol{s}}_k||^2}.\end{aligned}\tag{172}$$

As $N\to\infty$, from [1, Lemma 2.7] we have that (see also (27))

$$||\tilde{\boldsymbol{s}}_k||^2\xrightarrow{\text{a.s.}}Q\int_0^1\rho_k(x)dx\tag{173}$$

and, from Theorem 8.2, we have that conditioned on the fading

$$\tilde{\boldsymbol{s}}_k^\dagger\left(\frac{\mathsf{snr}}{Q}\tilde{\boldsymbol{S}}_k\tilde{\boldsymbol{S}}_k^\dagger+\boldsymbol{I}\right)^{-1}\tilde{\boldsymbol{s}}_k\xrightarrow{a.s.}Q\int_0^1\rho_k(x)v(x,\mathsf{snr})dx,\tag{174}$$

where $\rho_k(\cdot)$ is the one-dimensional channel profile function of the kth column of $\frac{1}{\sqrt{Q}}\boldsymbol{HA}$ and $v(\cdot,\mathsf{snr})$ is the solution to (22). From (172)–(174), the theorem follows.

C. Proof of Property 4.3

Denote by $\mathcal{I}_X$ the subset of $[0,1]$ such that

$$\mathcal{I}_X\equiv\{x\in[0,1]:\mathcal{Z}_X(x)\neq 0\}\tag{175}$$

and, analogously, denote by $\mathcal{I}_Y$ the subset of $[0,\beta]$ such that

$$\mathcal{I}_Y\equiv\{y\in[0,\beta]:\mathcal{Z}_Y(y)\neq 0\}\tag{176}$$

with $\mathcal{Z}_X(\cdot)$ and $\mathcal{Z}_Y(\cdot)$ defined in (37). If $y\in\overline{\mathcal{I}_Y}$ with $\overline{\mathcal{I}_Y}$ such that $\mathcal{I}_Y\cup\overline{\mathcal{I}}_Y\equiv[0,\beta]$, then by definition

$$\mathcal{Z}_Y(y)=\int_0^1\rho(x,y)dx=0.$$

This implies that

$$\int_{\overline{\mathcal{I}_Y}}\frac{\rho(x,y)}{1+\mathsf{snr}\mu(y,\mathsf{snr})}dy=0\tag{177}$$

from the nonnegativity of $\rho(x,y)\ \forall\ (x,y)\in[0,1]\times[0,\beta]$. Therefore,

$$\int_0^\beta\frac{\rho(x,y)}{1+\mathsf{snr}\mu(y,\mathsf{snr})}dy=\int_{\mathcal{I}_Y}\frac{\rho(x,y)}{1+\mathsf{snr}\mu(y,\mathsf{snr})}dy\tag{178}$$

and, analogously

$$\begin{aligned}&\int_0^1\frac{\rho(x,y')dx}{1+\mathsf{snr}\int_{\mathcal{I}_Y}\frac{\rho(x,y)}{1+\mathsf{snr}\mu(y,\mathsf{snr})}dy}\\&\qquad=\int_{\mathcal{I}_X}\frac{\rho(x,y')dx}{1+\mathsf{snr}\int_{\mathcal{I}_Y}\frac{\rho(x,y)}{1+\mathsf{snr}\mu(y,\mathsf{snr})}dy}.\end{aligned}\tag{179}$$

With that, (25) can be rewritten as

$$\mu(y',\mathsf{snr})=\int_{\mathcal{I}_X}\frac{\rho(x,y')dx}{1+\mathsf{snr}\int_{\mathcal{I}_Y}\frac{\rho(x,y)}{1+\mathsf{snr}\mu(y,\mathsf{snr})}dy}.\tag{180}$$

From (25) and (180) it follows that $\mu(y',\mathsf{snr})$ cannot diverge even for $\mathsf{snr}\to\infty$. Since $\mu(y',\mathsf{snr})\geq 0$, it further follows that, if $y'\in\overline{\mathcal{I}_Y}$, then $\mu(y',\mathsf{snr})=0\ \forall\ \mathsf{snr}$. If, instead, $y'\in\mathcal{I}_Y$, we distinguish two cases:

a) $\lim_{\mathsf{snr}\to\infty}\mu(y',\mathsf{snr})=\theta(y')=0$;

b) $\lim_{\mathsf{snr}\to\infty}\mu(y',\mathsf{snr})=\theta(y')>0$. In this case, it can be seen from (180) that $\theta(y')$ satisfies

$$\theta(y')=\int_{\mathcal{I}_X}\frac{\rho(x,y')dx}{1+\int_{\mathcal{I}_Y}\frac{\rho(x,y)}{\theta(y)}dy}.\tag{181}$$

Dividing both sides of (181) by $\theta(y')$, and integrating on $\mathcal{I}_Y$

$$\int_{\mathcal{I}_Y}dy'=\int_{\mathcal{I}_X}\frac{\int_{\mathcal{I}_Y}\frac{\rho(x,y')}{\theta(y')}dy'}{1+\int_{\mathcal{I}_Y}\frac{\rho(x,y)}{\theta(y)}dy}dx\tag{182}$$

which can be further manipulated into

$$\int_{\mathcal{I}_Y}dy=\int_{\mathcal{I}_X}\left(1-\frac{1}{1+\int_{\mathcal{I}_Y}\frac{\rho(x,y)}{\theta(y)}dy}\right)dx.\tag{183}$$

Using $\int_{\mathcal{I}_Y}dy=Z_Y$ and $\int_{\mathcal{I}_X}dx=Z_X$, we finally obtain that when

$$\lim_{\mathsf{snr}\to\infty}\mu(y,\mathsf{snr})=\theta(y)>0$$

then $\theta(y)$ is the solution to

$$Z_X-Z_Y=\int_{\mathcal{I}_X}\frac{1}{1+\int_{\mathcal{I}_Y}\frac{\rho(x,y)}{\theta(y)}dy}dx.\tag{184}$$

Let us now find the conditions, in terms of β, Z_X, and Z_Y, under which $\lim_{\mathsf{snr}\to\infty}\mu(y',\mathsf{snr})$ assumes either zero or nonzero values. Since $\theta(y')$ is a nonnegative function, it follows from (184) that

- if $Z_X-Z_Y<0$ (i.e., $Z_Y/Z_X>1$), the above fixed-point equation does not admit a solution. Thus, $\mu(y',\mathsf{snr})$ does not converge to a nonzero value as $\mathsf{snr}\to\infty$ and hence,
$$\lim_{\mathsf{snr}\to\infty}\mu(y',\mathsf{snr})=\theta(y')=0;$$
- if $Z_X=Z_Y$ (i.e., $Z_Y/Z_X=1$), then the only solution admitted by (184) is
$$\lim_{\mathsf{snr}\to\infty}\mu(y',\mathsf{snr})=\theta(y')=0;$$
- if $Z_X-Z_Y>0$ (i.e., $Z_Y/Z_X<1$), (184) admits a nonzero solution: consequently
$$\lim_{\mathsf{snr}\to\infty}\mu(y',\mathsf{snr})=\theta(y')>0$$
with $\theta(y')>0$ solution to (181). Moreover, for $Z_Y/Z_X<1$ the solution to (181) can be zero if and only if $\mathcal{Z}_Y(y')=0$ which implies, because of the uniqueness of the solution,

that $\mu(y',\mathsf{snr})$ itself is zero. In order to include this last scenario, we can rewrite (181) as

$$\theta(y') = \int_0^1 \frac{\rho(x,y')}{1+\int_0^\beta \frac{\rho(x,y)}{\theta(y)}dy}dx.$$

D. Proof of Property 4.4

From the proof of Property 4.3 we have that, if $y' \in \overline{\mathcal{I}_Y}$, then $\mu(y',\mathsf{snr}) = 0\ \forall\ \mathsf{snr}$. Hence, by continuity

$$\lim_{\mathsf{snr}\to\infty} \mathsf{snr}\mu(y',\mathsf{snr}) = 0, \qquad \text{if } y' \in \overline{\mathcal{I}_Y}.$$

If $y' \in \mathcal{I}_Y$, then we need to distinguish between $Z_Y/Z_X < 1$ and $Z_Y/Z_X \geq 1$. For $Z_Y/Z_X < 1$

$$\lim_{\mathsf{snr}\to\infty} \mu(y',\mathsf{snr}) = \theta(y')$$

with $\theta(y')$ the positive solution to (40). Thus, for $Z_Y/Z_X < 1$

$$\lim_{\mathsf{snr}\to\infty} \mathsf{snr}\mu(y',\mathsf{snr}) = \infty, \qquad \forall\ y' \in \mathcal{I}_Y.$$

Let us now study the behavior of $\mathsf{snr}\mu(y',\mathsf{snr})$ as $\mathsf{snr}\to\infty$ when $y' \in \mathcal{I}_Y$ and $Z_Y/Z_X \geq 1$. Using (180)

$$\mathsf{snr}\mu(y',\mathsf{snr}) = \int_{\mathcal{I}_X} \frac{\rho(x,y')dx}{\frac{1}{\mathsf{snr}}+\int_{\mathcal{I}_Y}\frac{\rho(x,y)}{1+\mathsf{snr}\mu(y,\mathsf{snr})}dy}. \tag{185}$$

Define

$$\theta_1(y') = \lim_{\mathsf{snr}\to\infty} \mathsf{snr}\mu(y',\mathsf{snr}).$$

From (185), under the assumption $\theta_1(y') > 0$, $\theta_1(y')$ must satisfy

$$\theta_1(y') = \int_{\mathcal{I}_X} \frac{\rho(x,y')dx}{\int_{\mathcal{I}_Y}\frac{\rho(x,y)}{1+\theta_1(y)}dy}. \tag{186}$$

After some algebra, (186) implies

$$Z_X = \int_{\mathcal{I}_Y} \frac{\theta_1(y)}{1+\theta_1(y)}dy \tag{187}$$

which can be written as

$$Z_Y - Z_X = \int_{\mathcal{I}_Y} \frac{1}{1+\theta_1(y)}dy. \tag{188}$$

If $Z_Y - Z_X > 0$ (i.e., $Z_Y/Z_X > 1$), then (186) admits a nonzero finite solution. If $Z_Y = Z_X$ (i.e., $Z_Y/Z_X = 1$), then (186) does not admit any finite solution and thus $\theta_1(y') = \infty$.

E. Proof of Property 4.5

Equation (25) can be written as

$$\mu(y',\mathsf{snr}) = \int_{\mathcal{I}_X} \frac{\rho(x,y')dx}{1+\int_{\mathcal{I}_Y}\frac{\rho(x,y)}{\frac{1}{\mathsf{snr}}+\mu(y,\mathsf{snr})}dy}. \tag{189}$$

Differentiating both sides with respect to snr

$$\dot\mu(y',\mathsf{snr}) = \int_{\mathcal{I}_X} \frac{\rho(x,y')dx}{\left(1+\int_{\mathcal{I}_Y}\frac{\rho(x,y)}{\frac{1}{\mathsf{snr}}+\mu(y,\mathsf{snr})}dy\right)^2} \cdot \int_{\mathcal{I}_Y} \frac{\rho(x,y)}{\left(\frac{1}{\mathsf{snr}}+\mu(y,\mathsf{snr})\right)^2}\left(\dot\mu(y,\mathsf{snr}) - \frac{1}{\mathsf{snr}^2}\right)dy. \tag{190}$$

After some algebra, (190) can be expressed in terms of quantities such as $\mu(\cdot,\mathsf{snr})$, $\mathsf{snr}\mu(\cdot,\mathsf{snr})$, and $\frac{\mathsf{snr}\dot\mu(\cdot,\mathsf{snr})}{\mu(\cdot,\mathsf{snr})}$. Properties 4.3 and 4.4, which give the limiting values of $\mu(\cdot,\mathsf{snr})$ and $\mathsf{snr}\mu(\cdot,\mathsf{snr})$ as $\mathsf{snr}\to\infty$, can then be applied to obtain the limiting value of $\frac{\mathsf{snr}\dot\mu(\cdot,\mathsf{snr})}{\mu(\cdot,\mathsf{snr})}$.

F. Proof of Theorem 5.1

First we note that, if $\mathsf{snr} = 0$

$$\mathsf{C}^{\mathsf{opt}}(0) = 0 \tag{191}$$

$$\mathsf{C}^{\mathsf{mmse}}(0) = 0 \tag{192}$$

$$\pi(y',0) = 0 \tag{193}$$

and thus (96) holds for $\mathsf{snr} = 0$. To prove the theorem, it is sufficient to show that the derivatives of both sides of (96) with respect to snr are equal. From (95), it follows that

$$\mathsf{C}^{\mathsf{opt}}(\mathsf{snr}) = \int \log_2(1+\mathsf{snr}\lambda)\,dG(\lambda) \tag{194}$$

where $G(\lambda)$ is the asymptotic empirical eigenvalue distribution of $\frac{1}{Q}\tilde{\boldsymbol{S}}\tilde{\boldsymbol{S}}^\dagger$. Therefore,

$$\dot{\mathsf{C}}^{\mathsf{opt}}(\mathsf{snr}) = \frac{d}{d\mathsf{snr}}\int \log_2(1+\mathsf{snr}\lambda)\,dG(\lambda) \tag{195}$$

$$= \frac{\log_2 e}{\mathsf{snr}}\left(1 - \int \frac{1}{1+\mathsf{snr}\lambda}dG(\lambda)\right). \tag{196}$$

Note that

$$\int \frac{1}{1+\mathsf{snr}\lambda}dG(\lambda) = \lim_{N\to\infty}\frac{1}{N}\mathrm{Tr}\left\{\left(\boldsymbol{I}+\frac{\mathsf{snr}}{Q}\tilde{\boldsymbol{S}}\tilde{\boldsymbol{S}}^\dagger\right)^{-1}\right\}. \tag{197}$$

Consequently, using Theorem 2.1 we have

$$\dot{\mathsf{C}}^{\mathsf{opt}}(\mathsf{snr}) = \frac{\log_2 e}{\mathsf{snr}}\left(1 - \int_0^1 v(x,\mathsf{snr})dx\right) \tag{198}$$

with $v(\cdot,\mathsf{snr})$ the solution to (22). From Theorem 8.2 (see also (22) and (25))

$$\mu(y',\mathsf{snr}) = \int_0^1 v(x,\mathsf{snr})\rho(x,y')dx. \tag{199}$$

Therefore, denoting

$$\pi(y',\mathsf{snr}) = \frac{\mathsf{snr}}{1+\mathsf{snr}\mu(y',\mathsf{snr})} \tag{200}$$

from (22) and (25), we have

$$1 - \int_0^1 v(x,\mathsf{snr})dx = \int_0^\beta \mu(y',\mathsf{snr})\pi(y',\mathsf{snr})dy'. \tag{201}$$

Differentiating $\mathsf{C}^{\mathsf{mmse}}$ in (24)

$$\dot{\mathsf{C}}^{\mathsf{mmse}}(\mathsf{snr}) = \log_2 e\int_0^\beta\left(\frac{\mu(y',\mathsf{snr})+\mathsf{snr}\dot\mu(y',\mathsf{snr})}{1+\mathsf{snr}\mu(y',\mathsf{snr})}\right)dy'$$

$$= \log_2 e\left(\frac{1}{\mathsf{snr}}\cdot\int_0^\beta \mu(y',\mathsf{snr})\pi(y',\mathsf{snr})dy' + \int_0^\beta \dot\mu(y',\mathsf{snr})\pi(y',\mathsf{snr})dy'\right). \tag{202}$$

From (198), (200), (202), and (201)

$$\dot{\mathsf{C}}^{\mathsf{opt}}(\mathsf{snr}) - \dot{\mathsf{C}}^{\mathsf{mmse}}(\mathsf{snr}) = -\log_2 e\cdot\int_0^\beta \dot\mu(y',\mathsf{snr})\pi(y',\mathsf{snr})dy'. \tag{203}$$

From (25) and (200), it can be verified that

$$\int_0^\beta \mu(y',\mathsf{snr})\dot{\pi}(y',\mathsf{snr})dy' = \int_0^1 \frac{\int_0^\beta \rho(x,y')\dot{\pi}(y',\mathsf{snr})dy'}{1+\int_0^\beta \rho(x,y')\pi(y',\mathsf{snr})dy'}dx. \quad (204)$$

The right-hand side of (204) is easily recognized as

$$\frac{1}{\log_2 e}\frac{d}{d\mathsf{snr}}\int_0^1 \log_2\left(1+\int_0^\beta \rho(x,y')\pi(y',\mathsf{snr})dy'\right)dx \quad (205)$$

and thus we get (206) and (207) at the bottom of the page, which completes the proof.

G. Proof of Proposition 4.1

Using (24) and Property 4.2

$$\dot{\mathsf{C}}^{\mathsf{mmse}}(0) = \frac{\beta}{\log_e 2} \quad (208)$$

$$\ddot{\mathsf{C}}^{\mathsf{mmse}}(0) = -\frac{1}{\log_e 2}\left(2\int_0^1\left(\int_0^\beta \rho(x,y)dy\right)^2 dx + \int_0^\beta\left(\int_0^1 \rho(x,y)dx\right)^2 dy\right) \quad (209)$$

and, therefore, from (47) we get (210) at the bottom of the page. In turn, S_∞^{mmse} is given by [23]

$$S_\infty^{\mathsf{mmse}} = \lim_{\mathsf{snr}\to\infty}\frac{\mathsf{snr}\dot{\mathsf{C}}^{\mathsf{mmse}}(\mathsf{snr})}{\log_2 e}. \quad (211)$$

From (24) and (48)

$$\begin{aligned} S_\infty^{\mathsf{mmse}} &= \lim_{\mathsf{snr}\to\infty}\mathsf{snr}\int_0^\beta \frac{\mu(y',\mathsf{snr})+\mathsf{snr}\dot{\mu}(y',\mathsf{snr})}{1+\mathsf{snr}\mu(y',\mathsf{snr})}dy' \\ &= \lim_{\mathsf{snr}\to\infty}\mathsf{snr}\int_{\mathcal{I}_Y} \frac{\mu(y',\mathsf{snr})+\mathsf{snr}\dot{\mu}(y',\mathsf{snr})}{1+\mathsf{snr}\mu(y',\mathsf{snr})}dy' \\ &= \lim_{\mathsf{snr}\to\infty}\int_{\mathcal{I}_Y}\frac{1+\frac{\mathsf{snr}\dot{\mu}(y',\mathsf{snr})}{\mu(y',\mathsf{snr})}}{1+\frac{1}{\mathsf{snr}\mu(y',\mathsf{snr})}}dy'. \end{aligned} \quad (212)$$

Invoking Properties 4.3–4.5, (50) follows immediately.

H. Proof of Proposition 5.1

From (95) we have that [35]

$$\ddot{\mathsf{C}}^{\mathsf{opt}}(0) = -\log_2 e \lim_{N\to\infty}\frac{1}{N}\left\|\frac{1}{Q}\tilde{\boldsymbol{S}}\tilde{\boldsymbol{S}}^\dagger\right\|^2.$$

From [14], the second moment of $\frac{1}{Q}\tilde{\boldsymbol{S}}\tilde{\boldsymbol{S}}^\dagger$ conditioned on the fading converges almost surely to

$$\begin{aligned} \frac{1}{N}\left\|\frac{1}{Q}\tilde{\boldsymbol{S}}\tilde{\boldsymbol{S}}^\dagger\right\|^2 &\to \lim_{N\to\infty}\frac{1}{N}\mathrm{Tr}\left\{\left(\frac{1}{Q}\boldsymbol{H}\boldsymbol{A}\boldsymbol{A}^\dagger\boldsymbol{H}^\dagger\right)^2\right\} \\ &\to \int_0^1\left(\int_0^\beta \rho(x,y)dy\right)^2 dx + \int_0^\beta\left(\int_0^1\rho(x,y)dx\right)^2 dy \end{aligned} \quad (213)$$

from which, using $\dot{\mathsf{C}}^{\mathsf{opt}}(0)=\beta$, (105) follows straightforwardly. In order to prove (106), let us consider the equality

$$\mathsf{snr}\frac{d\mathsf{C}^{\mathsf{opt}}}{d\mathsf{snr}} = \log_2 e\cdot\int_0^\beta \frac{\mathsf{snr}\mu(y,\mathsf{snr})}{1+\mathsf{snr}\mu(y,\mathsf{snr})}dy \quad (214)$$

which follows from (31) and (196). Note that, in the downlink, (214) admits the reformulation

$$\mathsf{snr}\frac{d\mathsf{C}^{\mathsf{opt}}}{d\mathsf{snr}} = \xi\frac{d\mathsf{C}^{\mathsf{mmse}}}{d\xi} \quad (215)$$

with $\xi=\mathsf{snr}\eta$. From (214)

$$S_\infty^{\mathsf{opt}} = \lim_{\mathsf{snr}\to\infty}\frac{\mathsf{snr}\dot{\mathsf{C}}^{\mathsf{opt}}(\mathsf{snr})}{\log_2 e} \quad (216)$$

$$= \lim_{\mathsf{snr}\to\infty}\int_0^\beta\frac{\mathsf{snr}\mu(y,\mathsf{snr})}{1+\mathsf{snr}\mu(y,\mathsf{snr})}dy. \quad (217)$$

Applying Property 4.4, (106) follows straightforwardly. Specializing the above steps to the downlink, we obtain (120) and (121).

ACKNOWLEDGMENT

The authors are indebted to Dr. Angel Lozano from Bell Labs for many valuable discussions and suggestions.

$$\begin{aligned} \dot{\mathsf{C}}^{\mathsf{opt}}(\mathsf{snr})-\dot{\mathsf{C}}^{\mathsf{mmse}}(\mathsf{snr}) &= -\log_2 e\int_0^\beta\left[\dot{\mu}(y',\mathsf{snr})\pi(y',\mathsf{snr})+\mu(y',\mathsf{snr})\dot{\pi}(y',\mathsf{snr})\right]dy' \\ &\quad+\frac{d}{d\mathsf{snr}}\int_0^1\log_2\left(1+\int_0^\beta\rho(x,y')\pi(y',\mathsf{snr})dy'\right)dx \end{aligned} \quad (206)$$

$$= \frac{d}{d\mathsf{snr}}\left[-\log_2 e\cdot\int_0^\beta\mu(y',\mathsf{snr})\pi(y',\mathsf{snr})dy' + \int_0^1\log_2\left(1+\int_0^\beta\rho(x,y')\pi(y',\mathsf{snr})dy'\right)dx\right] \quad (207)$$

$$S_0^{\mathsf{mmse}} = \frac{2\beta^2}{2\int_0^1\left(\int_0^\beta\rho(x,y)dy\right)^2dx+\int_0^\beta\left(\int_0^1\rho(x,y)dx\right)^2dy}. \quad (210)$$

REFERENCES

[1] Z. D. Bai and J. W. Silverstein, "No eigenvalues outside the support of the limiting spectral distribution of large dimensional sample covariance matrices," *Ann. Probab.*, vol. 26, pp. 316–345, Aug. 1998.

[2] P. Billingsley, *Probability and Measure*. New York: Wiley, 1986.

[3] J. M. Chaufray, P. Loubaton, and W. Hachem, "Asymptotic analysis of optimum and sub-optimum CDMA MMSE receivers," in *Proc. IEEE Int. Symp. Information Theory (ISIT'02)*, Lausanne, Switzerland, Jun./Jul. 2002, p. 189.

[4] C. Chuah, D. N. C. Tse, J. Kahn, and R. Valenzuela, "Capacity scaling in MIMO wireless systems under correlated fading," *IEEE Trans. Inf. Theory*, vol. 48, no. 3, pp. 637–650, Mar. 2002.

[5] M. Debbah, W. Hachem, P. Loubaton, and M. de Courville, "MMSE analysis of certain large isometric random precoded systems," *IEEE Trans. Inf. Theory*, vol. 49, no. 5, pp. 1293–1311, May 2003.

[6] M. Debbah, P. Loubaton, and M. de Courville, "The spectral efficiency of linear precoders," in *Proc. Information Theory Workshop*, Paris, France, Mar. 2003, pp. 90–93.

[7] ——, "Linear precoders for OFDM wireless communications with MMSE equalization: Facts and results," in *Proc. Eusipco*, Toulouse, France, Sep. 2002.

[8] V. L. Girko, *Theory of Random Determinants*. Boston, MA: Kluwer Academic, 1990.

[9] A. J. Grant and P. D. Alexander, "Random sequence multisets for synchronous code-division multiple-access channels," *IEEE Trans. Inf. Theory*, vol. 44, no. 7, pp. 2832–2836, Nov. 1998.

[10] A. Guionnet and O. Zeitouni, "Concentration of the spectral measure for large matrices," *Electron. Commun. Probab.*, vol. 5, pp. 119–136, 2000.

[11] W. Hachem, "Simple polynomial detectors for DS/CDMA downlink transmission on frequency-selective channels," *IEEE Trans. Inf. Theory*, vol. 50, no. 1, pp. 164–171, Jan. 2004.

[12] S. V. Hanly and D. N. C. Tse, "Resource pooling and effective bandwidths in CDMA networks with multiuser receivers and spatial diversity," *IEEE Trans. Inf. Theory*, vol. 47, no. 4, pp. 1328–1351, May 2001.

[13] S. Hara and R. Prasad, "Overview of multicarrier CDMA," *IEEE Commun. Mag.*, vol. 35, no. 12, pp. 126–133, Dec. 1997.

[14] L. Li, A. M. Tulino, and S. Verdú, "Design of reduced-rank MMSE multiuser detectors using random matrix methods," *IEEE Trans. Inf. Theory*, vol. 50, no. 6, pp. 986–1008, Jun. 2004.

[15] A. Lozano, A. Tulino, and S. Verdú, "High-SNR power offset in multiantenna communication," in *Proc. IEEE Int. Symp. Information Theory (ISIT'04)*, Chicago, IL, Jun. 2004, p. 288.

[16] V. A. Marcenko and L. A. Pastur, "Distribution of eigenvalues for some sets of random matrices," *Math. USSR-Sbornik*, vol. 1, pp. 457–483, 1967.

[17] R. R. Müller, "Multiuser receivers for randomly spread signals: Fundamental limits with and without decision-feedback," *IEEE Trans. Inf. Theory*, vol. 47, no. 1, pp. 268–283, Jan. 2001.

[18] M. J. M. Peacock, I. B. Collings, and M. L. Honig, "Asymptotic SINR analysis of single-user MC-CDMA in Rayleigh fading," in *Proc. Int. Symp. Spread Spectrum Techniques and Applications*, Prague, Czech Republic, Sep. 2002, pp. 338–342.

[19] ——, "Asymptotic spectral efficiency of LMMSE multi-user multi-signature MC-CDMA in frequency-selective Rayleigh fading," in *Proc. GLOBECOM*, San Francisco, CA, Dec. 2003, pp. 1882–1886.

[20] H. V. Poor and S. Verdú, "Probability of error in MMSE multiuser detection," *IEEE Trans. Inf. Theory*, vol. 43, no. 3, pp. 858–871, May 1997.

[21] J. G. Proakis, *Digital Communications*, 2nd ed. New York: McGraw-Hill, 1989.

[22] P. Rapajic, M. Honig, and G. Woodward, "Multiuser decision-feedback detection: Performance bounds and adaptive algorithms," in *Proc. 1998 Int. Symp. Information Theory*, Cambridge, MA, Aug. 1998, p. 34.

[23] S. Shamai (Shitz) and S. Verdú, "The effect of frequency-flat fading on the spectral efficiency of CDMA," *IEEE Trans. Inf. Theory*, vol. 47, no. 4, pp. 1302–1327, May 2001.

[24] D. Shlyankhtenko, "Random Gaussian band matrices and freeness with amalgamation," *Int. Math. Res. Note*, vol. 20, pp. 1013–1025, Aug. 1996.

[25] J. W. Silverstein and Z. D. Bai, "On the empirical distribution of eigenvalues of a class of large dimensional random matrices," *J. Multivariate Anal.*, vol. 54, pp. 175–192, 1995.

[26] D. N. C. Tse and S. V. Hanly, "Linear multiuser receivers: Effective interference, effective bandwidth and user capacity," *IEEE Trans. Inf. Theory*, vol. 45, no. 2, pp. 641–657, Mar. 1999.

[27] A. M. Tulino, A. Lozano, and S. Verdú, "Impact of correlation on the capacity of multi-antenna channels," Bell Labs Tech. Memo., ITD-03-44786F, 2003.

[28] A. M. Tulino, S. Verdú, and A. Lozano, "Capacity of antenna arrays with space, polarization and pattern diversity," in *Proc. 2003 IEEE Information Theory Workshop (ITW'03)*, Paris, France, Apr. 2003, pp. 324–327.

[29] A. M. Tulino and S. Verdú, "Random matrix theory and wireless communications," *Foundations and Trends in Commun. and Inf. Theory*, vol. 1, no. 1, 2004.

[30] R. Van Nee and R. Prasad, *OFDM for Wireless Multimedia Communications*. Norwood, MA: Artech House, 2000.

[31] M. K. Varanasi and T. Guess, "Optimum decision feedback multiuser equalization with successive decoding achieves the total capacity of the Gaussian multiple-access channel," in *Proc. Asimolar Conf.*, Pacific Grove, CA, Nov. 1997, pp. 1405–1409.

[32] ——, "Achieving vertices of the capacity region of the synchronous correlated-waveform multiple-access channel with decision-feedback receivers," in *Proc. IEEE Int. Symp. Information Theory*, Ulm, Germany, Jun. 1997, pp. 270–270.

[33] S. Verdú, *Multiuser Detection*. New York: Cambridge Univ. Press, 1998.

[34] ——, "Capacity region of Gaussian CDMA channels: The symbol-synchronous case," in *Proc. 24th Allerton Conf. Communications, Control and Computing*, Monticello, IL, Oct. 1986, pp. 1025–1034.

[35] ——, "Spectral efficiency in the wideband regime," *IEEE Trans. Inf. Theory*, vol. 48, no. 6, pp. 1319–1343, Jun. 2002.

[36] S. Verdú and S. Shamai (Shitz), "Spectral efficiency of CDMA with random spreading," *IEEE Trans. Inf. Theory*, vol. 45, no. 2, pp. 622–640, Mar. 1999.

[37] J. Zhang, E. K. P. Chong, and D. N. C. Tse, "Output MAI distributions of linear MMSE multiuser receivers in CDMA systems," *IEEE Trans. Inf. Theory*, vol. 47, no. 4, pp. 1128–1144, May 2001.